Table III. Mean domain scores for the principal domains.

JRQLQ			RQLQJ		
Domain	No. of items	Mean score (SD)	Domain	No. of items	Mean score (SD)
			New symptoms	4	3.04 (1.24)*
			Eye symptoms	4	2.14 (1.42)
Usual daily activities	5	1.48 (1.00)*	Activities conditions	3	3.04 (1.24)*
Outdoor activities	2	1.36 (1.00)*			
Social functioning	3	0.91 (0.94)			
Sleep problems	1	1.41 (1.29)*	Sleep problems	3	1.03 (1.72)
Emotional function	6	1.52 (1.29)	Emotional function	4	2.19 (1.37)
General health problems	2	1.36 (1.14)*	Non-nose/eye symptoms	7	2.06 (1.35)
			Practical problems	3	3.47 (1.57)*

*$p < 0.001$ (Kruskal–Wallis test).
Comparing mean scores for each domain with that for the social functioning domain in the JRQLQ and those for nose-symptoms activities limitation and practical problems with those for the other domains in the RQLQJ.

that the two questionnaires are comparable for the assessment of QOL.

To assess clinical validity, nose and eye symptom levels were investigated in relation to QOL domain scores. Nose and eye symptom domains correlated well with each other ($p < 0.001$). In the JRQLQ (Table VI), Spearman's correlation coefficients were >0.4 between most symptoms. In the RQLQJ, almost all nose and eye symptoms, with the exceptions of sore and swollen eyes, were correlated (>0.4; $p < 0.001$) with all domains (Table VI). These results indicate that nasal/ocular symptom levels correlated well with scores for individual domains and that the RQLQJ is probably more sensitive and more valid than the JRQLQ.

Overall scores also correlated well with all items and domains in both questionnaires, showing correlation coefficients of >0.4 (Table VI). These results suggest that both questionnaires have clinical validity.

The domain–domain correlation between the questionnaires was high (correlation coefficients of >0.4), showing that the questionnaires had similar constructions (Tables IV and V). The mean overall scores were also correlated with the scores for each domain similarly for both questionnaires, suggesting their similar constructions (Table V).

The JRQLQ items were grouped into six domains, indicating a few contradictions with the previous hypothesis [4,5]. Factors and their loadings in the JRQLQ are shown in Table VII. The total variance explained was 82.5%. The RQLQJ factor structure is shown in Table VIII. The RQLQJ showed a slightly scattered structure, as observed in a previous study [5,6], with a total variance explained of 71.9%.

In an item–domain multitrait analysis of the JRQLQ, the highest correlations were obtained within the same domain (Table IX). Similar results were seen for the RQLQJ, with a few contradictions. The runny nose item from nasal symptoms was more highly correlated with practical problems ($r = 0.744$), the blowing nose item from practical problems was more highly correlated with nasal symptoms ($r = 0.780$) and reduced productivity was more highly correlated with non-nose/eye symptoms ($r = 0.872$) (Table X). Both questionnaires showed satisfactory convergent and discriminate properties. Taken together with the factor and multitrait analyses, it was concluded that the construct of both questionnaires was satisfied.

Table IV. Correlations between domain scores for the two questionnaires. Values in bold indicate high Spearman's correlation coefficients in similar domains between the JRQLQ and the RQLQJ.

	JRQLQ					
RQLQJ	Daily activities	Outdoor	Social	Sleep problems	General health problems	Emotional function
Activities limitation	**0.653**	**0.586**	0.519	0.505	0.534	0.627
Sleep problems	0.454	0.409	0.337	**0.814**	0.533	0.521
Non-nose/eye symptoms	0.521	0.578	0.534	0.558	**0.741**	0.734
Practical problems	0.548	0.481	0.490	0.496	0.470	0.545
Nose symptoms	0.620	0.477	0.491	0.545	0.474	0.561
Eye symptoms	0.529	0.473	0.387	0.455	0.497	0.569
Emotional function	0.625	0.569	0.619	0.498	0.629	**0.797**

Table V. Correlations between the JRQLQ and RQLQJ in adjusted and matched domains.[a]

JRQLQ	RQLQJ	Pearson	Spearman
Nose symptoms	Nose symptoms	0.775	0.743
Eye symptoms	Eye symptoms	0.818	0.821
Usual daily activities	Activities limitation	0.653	0.664
Usual daily activities + outdoor activities	Activities limitation	0.685	0.698
Social functioning	Activities limitation	0.478	0.457
Sleep problems	Sleep problems	0.782	0.747
Emotional function	Emotional function	0.741	0.748
General health problems	Non-nose/eye symptoms	0.665	0.670
Usual daily activities	Non-nose/eye symptoms	0.740	0.748
Nose symptoms	Practical problems	0.670	0.585
Face scale	Overall RQLQJ	0.489	0.554
Total JRQLQ	Overall RQLQJ	0.797	0.773

[a]Scores for each domain on both questionnaires were significantly correlated ($p < 0.001$; Pearson's and Spearman's tests).

The internal consistency reliability of each domain in the two questionnaires was also satisfactory (Cronbach's alpha >0.76), indicating excellent reliability (Table XI).

There were no floor or ceiling effects.

Discussion

On the basis of this study it can be concluded that both the JRQLQ and RQLQJ are equally useful tools for the practical assessment of QOL in AR. They have good acceptability, excellent reliability and adequate construct validity. However, there are several differences between the questionnaires in terms of their construction. There are 6 domains in the JRQLQ and 7 in the RQLQJ; the total number of items is 18 and 28, respectively. In the JRQLQ, principal target domains were usual daily activity (38.8% of total items, including the outdoor activity domain), followed by social functioning and emotional function (17.4% each), with the exception of the nasal/ocular symptom domain, but there was no practical problem domain. In the RQLQJ, principal target domains were nasal/ocular symptoms (27.6%) and non-eye/nose symptoms (24.1%), followed by practical problems and emotional function (13.8% each), but there was no social functioning domain. Accordingly, it is characterized that the JRQLQ and RQLQJ mainly target usual daily activities and rhinitis-related health problems, respectively. QOL is a concept that includes a large set of physical, psychological, social and functional aspects of the

Table VI. Clinical validity: Correlation coefficients of symptoms levels with individual mean domain scores in the (a) JRQLQ and (b) RQLQJ. Values in bold indicate high correlation coefficients.

(a)

Domain	Runny nose	Sneezing	Stuffy nose	Itchy nose	Itchy eyes	Watery eyes
Usual daily activities	**0.577**	**0.507**	**0.420**	**0.399**	**0.407**	**0.400**
Outdoor activities	**0.453**	0.397	0.283	0.327	**0.391**	0.301
Social functioning	**0.408**	0.326	0.322	0.209	0.280	0.263
Sleep problems	0.387	0.390	**0.511**	0.349	0.350	0.334
General health problems	0.396	0.380	0.349	0.387	0.365	0.340
Emotional function	**0.459**	**0.421**	0.335	**0.416**	0.388	0.335
Overall	**0.555**	**0.496**	**0.430**	**0.426**	**0.440**	**0.406**

(b)

Domain	Runny nose	Sneezing	Stuffy nose	Itchy nose	Itchy eyes	Watery eyes	Sore eyes	Swollen eyes
Activities limitation	**0.458**	**0.594**	**0.560**	**0.534**	**0.478**	**0.434**	0.395	**0.440**
Sleep problems	**0.537**	0.378	**0.409**	**0.466**	**0.464**	**0.378**	0.384	0.388
Non-nose/eye symptoms	**0.470**	**0.531**	**0.491**	**0.540**	**0.481**	**0.526**	**0.517**	**0.561**
Practical problems	**0.504**	**0.751**	**0.668**	**0.596**	**0.594**	**0.526**	0.386	**0.440**
Nose symptoms	**0.758**	**0.854**	**0.767**	**0.835**	**0.460**	**0.532**	0.375	**0.414**
Eye symptoms	0.337	**0.416**	**0.468**	**0.519**	**0.811**	**0.826**	**0.828**	**0.843**
Emotional function	**0.409**	**0.536**	**0.517**	**0.532**	**0.531**	**0.607**	**0.504**	**0.515**
Overall	**0.606**	**0.701**	**0.669**	**0.702**	**0.663**	**0.677**	**0.605**	**0.642**

Table VII. Factor analysis for the JRQLQ. Values in bold indicate high correlation coefficients.

Item	Factor					
	F1	F2	F3	F4	F5	F6
Reduced productivity	0.258	0.248	**0.816**	0.152	0.212	0.114
Poor mental concentration	0.337	0.405	**0.684**	0.249	0.120	0.274
Reduced thinking power	0.250	0.555	**0.589**	0.283	0.106	0.211
Impaired reading	0.217	**0.737**	0.333	0.202	0.212	0.103
Poor memory	0.261	**0.769**	0.207	0.168	0.239	0.167
Limitation of outdoor life	0.211	0.356	0.123	**0.757**	0.109	0.220
Limitation of going out	0.313	0.133	0.249	**0.781**	0.257	0.182
Reluctance to visit friends	0.282	0.096	0.240	0.569	**0.577**	0.116
Reduced contact with friends	0.149	0.227	0.205	0.326	**0.744**	0.241
Uneasy with people around you	0.300	0.196	0.072	0.054	**0.832**	0.093
Impaired sleeping	0.210	0.235	0.083	0.148	0.207	**0.820**
Tiredness	0.567	0.045	0.315	0.276	0.118	**0.603**
Fatigue	0.525	0.101	0.305	0.248	0.112	**0.629**
Frustrated	**0.746**	0.180	0.310	0.259	0.184	0.308
Irritable	**0.795**	0.251	0.265	0.118	0.222	0.190
Depressed	**0.880**	0.197	0.194	0.158	0.273	0.155
Unhappy	**0.680**	0.360	0.059	0.277	0.239	0.236
Loading rate (%)	21.6%	13.2%	12.5%	12.4%	11.6%	11.2%

lives of healthy or ill patients [10]. Although many definitions of QOL have been proposed, the JRQLQ includes all essential domains.

Scores from nose and eye symptoms were excluded from the total QOL score for the JRQLQ but were included in the overall RQLQJ score, because

Table VIII. Factor analysis for the RQLQJ. Values in bold indicate high correlation coefficients.

Item	Factor						
	F1	F2	F3	F4	F5	F6	F7
Activities limitation	0.217	0.208	0.215	0.159	**0.735**	0.003	0.207
	0.440	0.284	0.039	0.054	0.395	0.089	0.395
	0.363	0.403	0.115	0.208	**0.480**	0.0036	0.209
Difficulty getting to sleep	0.258	0.172	0.165	**0.707**	0.145	0.099	0.223
Waking up during night	0.179	0.179	0.131	**0.859**	0.120	0.087	0.079
Lack of a good night's sleep	0.241	0.197	0.166	**0.867**	0.143	0.091	0.097
Tiredness	**0.724**	0.224	0.182	0.192	0.176	0.211	0.100
Fatigue	**0.664**	0.134	0.218	0.193	0.194	0.010	0.117
Thirst	0.498	0.105	0.172	0.352	0.004	0.128	**0.558**
Reduced productivity	**0.761**	0.260	0.237	0.159	0.260	0.163	0.032
Poor concentration	**0.774**	0.251	0.272	0.143	0.291	0.119	0.079
Headache	0.322	0.109	0.169	0.241	0.065	**0.641**	0.245
Worn out	**0.719**	0.206	0.201	0.270	0.046	0.333	0.077
Inconvenience of carrying tissues	0.103	**0.794**	0.154	0.205	0.016	0.218	0.039
Need to rub nose/eyes	0.234	**0.633**	0.448	0.302	0.157	0.092	0.090
Need to blow nose repeatedly	0.233	**0.835**	0.110	0.145	0.112	0.164	0.147
Stuffy nose	0.060	0.356	0.066	0.399	0.165	0.181	**0.586**
Runny nose	0.254	**0.790**	0.046	0.042	0.221	0.121	0.262
Sneezing	0.220	**0.664**	0.117	0.153	0.297	0.117	0.058
Postnasal drip	0.136	**0.502**	0.290	0.180	0.202	0.213	0.425
Itchy eyes	0.163	0.370	**0.653**	0.299	0.247	0.003	0.180
Watery eyes	0.198	0.344	**0.642**	0.109	0.225	0.196	0.032
Sore eyes	0.234	0.051	**0.782**	0.135	0.129	0.115	0.163
Swollen eyes	0.287	0.112	**0.783**	0.083	0.064	0.159	0.217
Frustrated	0.299	0.337	0.252	0.213	**0.540**	0.359	0.159
Irritable	0.456	0.264	0.256	0.190	**0.598**	0.285	0.057
Impatient restless	0.383	0.041	0.362	0.146	**0.464**	0.464	0.050
Embarrassed	0.138	0.313	0.120	0.020	0.172	**0.771**	0.061
Loading rate (%)	16.4	11.9	10.9	12.0	8.8	6.7	5.2

Table IX. Convergent and discriminate validity, multitrait item–domain analysis for the JRQLQ.[a]

Item	Domain					
	Usual daily activities	Outdoor activities	Social functioning	Sleep problems	General health problems	Emotional function
Work	**0.842**	0.538	0.499	0.411	0.520	0.586
Mental	**0.924**	0.630	0.536	0.507	0.652	0.694
Thinking	**0.912**	0.593	0.514	0.417	0.581	0.602
Reading	**0.828**	0.551	0.522	0.402	0.449	0.556
Memory	**0.779**	0.505	0.571	0.414	0.523	0.572
Outdoor	0.595	**0.925**	0.574	0.437	0.530	0.545
Going out	0.612	**0.921**	0.700	0.441	0.613	0.642
Friends	0.554	0.681	**0.886**	0.388	0.553	0.599
Communication	0.574	0.599	**0.903**	0.447	0.509	0.542
Uneasy with people	0.455	0.463	**0.794**	0.343	0.413	0.516
Sleep	0.501	0.474	0.441	**1.00**	0.608	0.560
Tiredness	0.616	0.613	0.565	0.597	**0.980**	0.777
Fatigue	0.618	0.600	0.552	0.591	**0.974**	0.737
Frustration	0.686	0.619	0.588	0.548	0.786	**0.941**
Irritable	0.663	0.582	0.581	0.495	0.721	**0.932**
Depressed	0.576	0.553	0.566	0.489	0.654	**0.895**
Unhappy	0.558	0.575	0.586	0.524	0.624	**0.832**

[a]Stronger relationships (bold face) with same measures and weaker relationships (standard face) with different measures suggest good convergent and discriminate validity.

Table X. Convergent and discriminate validity, multitrait item domain correlation for the RQLQJ.[a]

Item	Domain						
	Activities limitation	Sleep problems	Non-nose/eye symptoms	Practical problems	Nose symptoms	Eye symptoms	Emotional functions
Activity 1	**0.775**	0.406	0.624	0.444	0.543	0.393	0.543
Activity 2	**0.838**	0.459	0.598	0.553	0.581	0.451	0.545
Activity 3	**0.830**	0.422	0.531	0.427	0.507	0.492	0.583
Sleep 1	0.478	**0.819**	0.553	0.444	0.555	0.434	0.451
Sleep 2	0.463	**0.921**	0.521	0.440	0.461	0.432	0.423
Sleep 3	0.523	**0.954**	0.592	0.511	0.535	0.489	0.497
Tiredness	0.623	0.485	**0.829**	0.478	0.527	0.528	0.639
Thirst	0.522	0.546	**0.727**	0.382	0.503	0.429	0.407
Reduced productivity	0.644	0.492	**0.872**	0.514	0.537	0.600	**0.688**
Sleepy	0.499	0.463	**0.744**	0.372	0.434	0.499	0.517
Mental concentration	0.671	0.494	**0.893**	0.514	0.559	0.614	0.697
Headache	0.363	0.390	0.595	0.362	0.449	0.344	0.417
Fatigue	0.610	0.526	**0.863**	0.512	0.525	0.524	0.608
Carrying tissues	0.486	0.423	0.432	**0.914**	0.656	0.436	0.491
Rubbing nose	0.580	0.532	0.577	**0.870**	0.634	0.601	0.589
Blowing nose	0.542	0.432	0.536	**0.893**	**0.780**	0.451	0.544
Stuffy nose	0.468	0.529	0.460	0.508	**0.751**	0.337	0.394
Runny nose	0.594	0.397	0.528	**0.744**	**0.856**	0.397	0.525
Sneezing	0.551	0.414	0.499	0.639	**0.749**	0.478	0.516
Pestnasal drip	0.581	0.478	0.552	0.605	**0.841**	0.536	0.534
Itchy eyes	0.477	0.475	0.485	0.567	0.441	**0.825**	0.533
Watery eyes	0.433	0.390	0.527	0.514	0.529	**0.826**	0.595
Sore eyes	0.414	0.381	0.502	0.389	0.373	**0.800**	0.497
Swollen eyes	0.471	0.353	0.565	0.406	0.395	**0.798**	0.506
Frustrated	0.593	0.473	0.608	0.553	0.545	0.609	**0.862**
Irritable	0.664	0.502	0.707	0.541	0.579	0.601	**0.896**
Impatient	0.550	0.418	0.647	0.420	0.441	0.587	**0.840**
Embarrassed	0.395	0.285	0.427	0.486	0.436	0.388	**0.685**

[a]Stronger relationships (bold face) were seen within the similar domains. Weaker relationships (standard face) were seen between different domains.

Table XI. Reliability, internal consistency reliability.

Domain	Cronbach's alpha
JRQLQ	0.916
Usual daily activities	0.839
Outdoor activities	0.844
Social functioning	
Sleep problems	
General health problems	0.954
Emotional function	0.936
RQLQJ	
Activities limitation	0.736
Sleep problems	0.900
Non-nose/eye symptoms	0.906
Practical problems	0.870
Nose symptoms	0.813
Eye symptoms	0.846
Emotional function	0.843

impairment of QOL results from nose/eye symptoms, but these symptoms do not represent QOL itself. In the RQLQJ, 8/28 items (28.5%) refer to nose and eye symptoms, which greatly affects the total score. However, if required, the nose and eye symptom scores in the JRQLQ could be included in the overall total QOL score, as with the RQLQJ, or totalized separately from the total QOL score, as with the JRQLQ.

In the activity limitation domain in the RQLQJ, patients select only three items from a list of example items. This number would seem to be too small, compared with the three items in the sleep problem domain and the seven items in the non-nose/eye symptoms domain. The three items in the sleep problem domain were highly correlated with each other and these three items may be sufficient for Japanese subjects. The items in the practical problem domain also overlap directly with those for nose symptoms. If the number of items in these two domains were reduced, the RQLQJ might become simpler. The correlation of symptom scores within each domain was better in the RQLQJ than the JQRQL. This suggests that the RQLQJ may be more responsive to changes in symptomatology due to the greater number of options in the response continuum [9].

In the JQRQL, nose and eye symptom scores were separated from QOL scores, because QOL impairment results from nose/eye symptoms but these symptoms do not represent QOL itself.

In a pilot study of 100 patients with JCP at the Japan Allergy and Asthma Clinic, the major nose/eye symptoms were runny nose (95%), sneezing (80%), stuffy nose (77%), itchy nose (28%), itchy eyes (80%) and watery eyes (29%). In contrast to Juniper's questionnaire [2], postnasal drip (21%) and eye swelling (9%) were mentioned infrequently and eye pain was not mentioned at all. There may be differences in lifestyle, habits, behavior and characteristics of pollinosis from country to country. The eye pain item in the RQLQJ may have been a mistranslation into Japanese from the original English version of the RQLQ. Thus, symptoms in the JRQLQ consisted of runny nose, sneezing, stuffy nose, itchy nose, itchy eyes and watery eyes. In the RQLQJ, postnasal drip, sore eyes and swollen eyes were added to the nose and eye symptoms included in the JRQLQ in accordance with Juniper's original questionnaire (Table II).

Conclusions

Both the JRQLQ and RQLQJ are useful instruments for the assessment of QOL in rhinoconjunctivitis due to JCP, and possibly in other forms of seasonal rhinitis in Japan, on the basis of their similar psychometric performance. The questionnaires differ from each other in terms of their linguistic expression and response options for items and deal differently with nasal–ocular symptom scores. This may be due to differences in lifestyle, and the types of allergens also differ between Japan and Western countries. However, both questionnaires were demonstrated to be comparable and equally useful for the assessment of QOL in rhinoconjunctivitis. When compared with each other, the JRQLQ focuses on usual daily activities and is simpler and faster to complete, whilst the RQLQJ concentrates on pollinosis-related health problems, has more overlap between domains and is more responsive. Thus, after completion of linguistic and cultural adaptation and validation, the JRQLQ may become available in other countries in addition to the RQLQJ.

Acknowledgements

The authors express their thanks to Ono Pharmaceutical and Aventis for their financial support and help with the statistical analyses.

References

[1] Van Wijk RG. A global problem: quality of life. Allergy 2002;57:1097–110.
[2] Juniper EF. Measuring health-related quality of life in rhinitis. J Allergy Clin Immunol 1997;99S:742–9.
[3] Crawford B, Okuda M. Psychometric validation of a Japanese translated RQLQ and WPAI-As [Abstract]. J Allergy Clin Immunol 2003;111:S175.
[4] Okuda M, Crawford B, Juniper E, Leathy M. Japanese translated RQLQ and WPAI-AS. Jpn J Allergology 2003;52(Suppl 1):70–86.

[5] Okuda M, Ohkubo K, Goto M, Okamoto Y, Konno A, Baba K, et al. Japanese allergic rhinitis quality of life questionnaire. Jpn J Allergology 2003;52(Suppl 1):21–56.
[6] Fitzpatrick R, Flecher A, Gore S, Spiegelhalten D, Cox D. Quality of life measures in health care. Br Med J 1992;305:1074–7.
[7] Gandek B, Ware JE. Methods for validating and norming translation of health status questionnaires. J Clin Epidemiol 1998;51:953–8.
[8] Armitage P, Berry G, Mathews JNS. Multivariate methods. Statistical methods in medical research. Oxford, UK: Blackwell Science; 2002. p. 455–83.
[9] Ware JE, Gandek B. Methods for testing data quality, scaling assumption, and reliability: the IQOLA project approach. J Clin Epidemiol 1998;11:945–52.
[10] Walker SR, Rossen RM. Quality of life: assessment and application. Ciba Found Symp 1978;169–78.

Int. J. Cancer: **117,** 265–273 (2005)

Dendritic cell maturation by CD11c$^-$ T cells and Vα24$^+$ natural killer T-cell activation by α-Galactosylceramide

Eiichi Ishikawa[1,2], Shinichiro Motohashi[2,3], Aki Ishikawa[2,3], Toshihiro Ito[2], Tetsuro Uchida[2,4], Takaaki Kaneko[2], Yuriko Tanaka[2,4], Shigetoshi Horiguchi[4], Yoshitaka Okamoto[4], Takehiko Fujisawa[3], Koji Tsuboi[1], Masaru Taniguchi[5], Akira Matsumura[1] and Toshinori Nakayama[2]*

[1]*Department of Neurosurgery, Institute of Clinical Medicine, University of Tsukuba, Tsukuba Science City, Ibaraki, Japan*
[2]*Department of Immunology, Graduate School of Medicine, Chiba University, Chuo-ku, Chiba, Japan*
[3]*Department of Thoracic Surgery, Graduate School of Medicine, Chiba University, Chuo-ku, Chiba, Japan*
[4]*Department of Otorhinolaryngology, Graduate School of Medicine, Chiba University, Chuo-ku, Chiba, Japan*
[5]*Laboratory for Immune Regulation, Riken Research Center for Allergy and Immunology, Yokohama, Japan*

Human invariant Vα24$^+$ natural killer T (NKT) cells display potent antitumor activity upon stimulation. Activation of endogenous Vα24$^+$ NKT cells would be one strategy for the treatment of cancer patients. For example, dendritic cells (DCs) loaded with a glycolipid NKT cell ligand, α-galactosylceramide (αGalCer, KRN7000), are a possible tool for the activation and expansion of functional Vα24$^+$ NKT cells *in vivo*. In this report, we demonstrate that the levels of expansion and the ability to produce IFN-γ of Vα24$^+$ NKT cells induced by αGalCer-loaded whole PBMCs cultured with IL-2 and GM-CSF (IL-2/GM-CSF-cultured PBMCs) were superior to those of cells induced by monocyte-derived CD11c$^+$ DCs (moDCs) developed with IL-4 and GM-CSF. Interestingly, CD11c$^+$ cells in the IL-2/GM-CSF-cultured PBMCs showed a mature phenotype without further stimulation and exerted potent stimulatory activity on Vα24$^+$ NKT cells to enable them to produce IFN-γ preferentially at an extent equivalent to mature moDCs induced by stimulation with LPS or a cytokine cocktail. Cocultivation with CD11c$^-$ cells in the IL-2/GM-CSF-cultured PBMCs induced maturation of moDCs. In particular, CD11c$^-$CD3$^+$ T cells appeared to play important roles in DC maturation. In addition, TNF-α was preferentially produced by CD11c$^-$CD3$^+$ T cells in IL-2/GM-CSF-cultured PBMCs and was involved in the maturation of moDCs. Thus, the maturation of DCs induced by CD11c$^-$ T cells through TNF-α production appears to result in the efficient expansion and activation of Vα24$^+$ NKT cells to produce IFN-γ preferentially.

Key words: natural killer T cell; α-galactosylceramide; granulocyte/macrophage colony-stimulating factor; peripheral blood mononuclear cell; immunotherapy

Murine Vα14$^+$ NKT cells, characterized by expression of a single invariant receptor encoded by the Vα14 and Jα281 gene segments, have been identified as a novel lymphocyte lineage.[1–5] Upon stimulation with a glycolipid, αGalCer, Vα14$^+$ NKT cells assume various functions, including the ability to regulate cytokine-mediated Th1/Th2 differentiation and perforin/granzyme B-mediated antitumor activity.[2,4,6,7] In addition, a significant role of Vα14$^+$ NKT cells in tumor surveillance has been suggested.[6] Human Vα24$^+$ NKT cells bearing the invariant receptors Vα24JaQ and Vβ11, the counterpart of murine Vα14$^+$ NKT cells, also recognize αGalCer in a CD1d-dependent fashion[8] and display potent antitumor activity *in vitro*.[9–13] A series of promising results in studies of the antitumor effects of activated Vα14$^+$ NKT cells in murine tumor metastasis models[14–17] and the recognition of the same ligand, αGalCer, by human Vα24$^+$ NKT cells[9–13] encouraged us to establish an effective new approach to cancer immunotherapy using the αGalCer/CD1d-Vα24$^+$ NKT cell system as a target.

For clinical trials aimed at Vα24$^+$ NKT cell activation in cancer patients, a simple procedure would be to inject soluble αGalCer i.v. into cancer patients to activate endogenous Vα24$^+$ NKT cells. However, results in murine models indicated that αGalCer treatment was no longer effective when αGalCer treatment started 3 days after melanoma cell injection.[14,17] Moreover, multiple injections of soluble αGalCer induced an anergy state in NKT cells in murine tumor-bearing models[18,19] or a shift from Th1- to Th2-type cytokine production.[20,21] Indeed, a phase I clinical study involving i.v. injection of αGalCer into advanced cancer patients resulted in neither Vα24$^+$ NKT cell expansion nor clinical responses, although feasibility was proved.[22] Several investigators, including us, have noted that DCs expressing CD1d present αGalCer efficiently to murine Vα14 and human Vα24 NKT cells. We reported that in a murine tumor-metastasis model, αGalCer-loaded DCs showed potent antitumor activity that eradicated multiple small metastatic nodules generated in the liver.[14] It was shown that injection of αGalCer-loaded DCs induced prolonged IFN-γ production in NKT cells.[18] The results of a clinical study using IL-4 and GM-CSF–cultured DCs loaded with αGalCer suggested the feasibility of the procedure.[23,24] Thus, inducing the activation and expansion of endogenous Vα24$^+$ NKT cells by αGalCer-loaded DCs would be a promising strategy for cancer immunotherapy.

In tumor immunotherapy using DCs loaded with tumor peptides, plastic-adherent or CD14$^+$ PBMCs were cultured with GM-CSF and IL-4 to cause them to differentiate into DCs,[25,26] which were recently refined for clinical application.[27] Since the frequency of Vα24$^+$ NKT cells is very low (<0.3% of PBMCs), very large numbers of CD1d-expressing APCs would be required to induce efficient activation and expansion of endogenous Vα24$^+$ NKT cells. However, it is very difficult to obtain large numbers of moDCs by standard procedures, making an alternative APC preparation method a necessity. In fact, CD1d expression is inducible on human T cells upon activation, although it has not been clarified whether activated CD1d-expressing T cells present αGalCer to human Vα24$^+$ NKT cells.[28–30]

Abbreviations: APC, antigen-presenting cell; DC, dendritic cell; αGalCer, α-galactosylceramide; GM-CSF, granulocyte/macrophage colony-stimulating factor; HV, healthy volunteer; LPS, lipopolysaccharide; MAb, monoclonal antibody; MACS, magnetic cell sorting; ME, mercaptoethanol; MFI, mean fluorescence intensity; moDC, monocyte-derived CD11c$^+$ DC; NKT, natural killer T; PBMC, peripheral blood mononuclear cell; PE, phycoerythrin; PGE_2, prostaglandin E_2; rh, recombinant human; TGF, transforming growth factor; TNF, tumor necrosis factor.

Grant sponsor: Ministry of Education, Culture, Sports, Science and Technology (Japan); Grant numbers: 13218016, 16043211, 14370107, 16616003, 15790248; Grant sponsor: Ministry of Health, Labor and Welfare (Japan); Grant sponsor: Program for Promotion of Fundamental Studies in Health Science of the Organization for Pharmaceutical Safety and Research (Japan); Grant sponsor: Cancer Translational Research Project; Grant sponsor: Japan Health Science Foundation; Grant sponsor: Uehara Memorial Foundation; Grant sponsor: Mochida Foundation.

***Correspondence to:** Department of Immunology, Graduate School of Medicine, Chiba University, 1-8-1 Inohana, Chuo-ku, Chiba 260-8670, Japan. Fax: +81-43-227-1498. E-mail: tnakayama@faculty.chiba-u.jp

Received 15 November 2004; Accepted after revision 23 March 2005
DOI 10.1002/ijc.21197
Published online 17 May 2005 in Wiley InterScience (www.interscience.wiley.com).

The results shown here indicate that αGalCer-loaded, IL-2/GM-CSF-cultured PBMCs induce very efficient expansion of autologous Vα24$^+$ NKT cells, which maintain the ability to produce IFN-γ compared to moDCs. Interestingly, the maturation of DCs induced by CD11c$^-$ T cells through TNF-α production appeared to be critical for the efficient activation of Vα24$^+$ NKT cells.

Material and methods

Cell preparation and culture of APCs including IL-2/GM-CSF-cultured PBMCs and moDCs

Written informed consent was obtained from HV1 and HV2 before sampling PBMCs. PBMCs were separated by density gradient centrifugation, washed once with PBS and twice with PBS (or RPMI-1640) supplemented with 3% heat-inactivated FBS and then used for experiments. The frequency of Vα24$^+$ NKT cells in PBMCs was 0.18% in HV1 and 0.008% in HV2. Vα24$^+$ NKT cells were defined as Vα24$^+$Vβ11$^+$ cells.[13,31]

For preparing IL-2/GM-CSF-cultured PBMCs, whole PBMCs were cultured for 7 days in the presence of rhIL-2 (100 JRU/ml; Imunace, Shionogi, Japan) and rhGM-CSF (800 U/ml; NCPC Gene Tech Biotechnology Development, Shi jiazhuang, People's Republic of China) in RPMI-1640 supplemented with 10% FBS, 0.01 mM 2-ME and 50 U/ml penicillin-streptomycin. For the preparation of moDCs, whole PBMCs were allowed to adhere to culture flasks for 1.5–2 hr at 37°C, and then adherent cells were cultured for 5–7 days in the presence of rhIL-4 (500 U/ml, R&D Systems, Minneapolis, MN) and rhGM-CSF (800 U/ml). CD11c$^+$ cells were purified by using a MACS separation column (Miltenyi Biotech, Bergisch Gladbach, Germany) according to the manufacturer's protocol. Briefly, moDCs or IL2/GM-CSF-cultured PBMCs were incubated with PE-conjugated anti-CD11c MAb (Pharmingen, La Jolla, CA) for 15 min, washed twice and then incubated with microbeads conjugated with anti-PE MAb (Miltenyi Biotech) for 30 min on ice in PBS containing 3% FBS. Magnetically labeled cells were applied to the auto-MACS apparatus, and trapped cells (the positive-selected fraction) and untrapped cells (the negative-selected fraction) were used as APCs. In the positive-selected fraction, >88% of cells were CD11c$^+$. CD11c$^-$ cells were purified from the nonadherent fraction of IL-2/GM-CSF-cultured PBMCs by depleting macrophages and adherent CD11c$^+$ cells using the MACS separation column. CD11c$^+$ cells accounted for <5% of the cells in the negative-selected fraction. The CD11c$^-$ cells contained marginal numbers (<1%) of macrophages (CD11b$^+$CD11c$^-$/low cells), NKT cells (Vα24$^+$Vβ11$^+$ cells), myelomonocytic cells (CD14$^+$CD3$^-$) and B cells (CD19$^+$CD3$^-$ cells), as well as CD11c$^+$ DCs. Mature CD11c$^+$ moDCs were obtained by culturing immature CD11c$^+$ moDCs with LPS (1,000 ng/ml), cytokine cocktail (IL-1β, 10 ng/ml; TNF-α, 10 ng/ml; and PGE_2, 1 μg/ml), PGE_2 (5 μg/ml) plus LPS (100 ng/ml) or OK432 (0.1 KE/ml) for 1–3 days.

Expansion and detection of Vα24$^+$ NKT cells

αGalCer (KRN7000) was provided by Kirin Brewery (Gunma, Japan) and prepared as described previously.[16] To detect Vα24$^+$ NKT cell expansion, APCs were loaded with αGalCer (100 ng/ml) or vehicle for 12–18 hr at 37°C in a 5% CO_2 incubator. Autologous PBMCs (0.2 to 1 × 10^6) prepared from the same volunteer were cultured for 6 days in the presence of various types of APC. Flow cytometry to detect Vα24$^+$Vβ11$^+$ cells was performed on an EPICS-XL flow cytometer (Beckman Coulter, Fullerton, CA), and the results were analyzed by Flow JO software (Tree Star, Inc., Ashland, OR). Vα24$^+$ NKT cell expansion was quantified by the following formula: NKT fold expansion = (whole live cell count after culture × % of NKT cells after culture)/(whole live cell count before culture × % of NKT cells before culture). For the NKT cell proliferation assay using [^{3}H]-thymidine, *in vitro* activated Vα24$^+$ NKT cells, prepared by 2 cycles of cultivation with IL-2 and αGalCer for 7 days, were stimulated with irradiated APCs for 72 hr at 37°C, with 0.5 μCi/well of [^{3}H]-thymidine added to the stimulation culture for the final 16 hr. Incorporated radioactivity was measured by a β-plate scintillation counter.

Flow-cytometric analysis

In general, 0.2 to 1 × 10^6 cells were stained with antibodies according to the standard method described previously.[9,13] The antibodies used were as follows: anti-Vα24-FITC (C15) and anti-Vβ11-PE (C21) (Coulter-Immunotech, Miami, FL) and anti-HLA-DR-FITC, anti-CD4-FITC, anti-CD56-FITC, anti-CD83-FITC, anti-CD11c-PE, anti-CD80-PE, anti-CD8-PE, anti-CD16-PE, anti-CD1d-PE, anti-CD86-Cy and anti-CD3-Cy (Pharmingen). For intracellular staining, anti-Vα24-biotin (C15, Coulter-Immunotech), anti-streptavidin-Cy-Chrome, an FITC-conjugated anti-IFN-γ antibody and a PE-conjugated anti-IL-4 antibody (Pharmingen) were used. For neutralization, anti-TNF-α (MABTNF-A5), anti-IFN-γ (NIB42), anti-IL-4 (MP4-25D2), anti-IL-12 (C8.6), anti-CD1d (CD1d42) or anti-MHC-I (G46-2.6) antibodies were purchased (Pharmingen). Different lymphocyte subsets were defined as follows: CD11c$^+$ DCs, SS^{high}FS^{high}CD11c$^+$ cells; CD4$^+$ T cells, SS^{low}FS^{low}CD4$^+$CD8$^-$CD3$^+$ cells; CD8$^+$ T cells, SS^{low}FS^{low}-CD4$^-$CD8$^+$CD3$^+$ cells; NK cells, SS^{low}FS^{low}CD56$^+$CD16$^+$CD3$^-$ cells; and NKT cells, SS^{low}FS^{low}Vα24$^+$Vβ11$^+$CD3$^+$ cells.

ELISAs for detecting cytokines in culture supernatants and ELISpot assays for detecting IFN-γ-producing Vα24$^+$ NKT cells

Concentrations (pg/ml) of IL-4 and IFN-γ in the culture supernatants derived from 2 × 10^5 cell cultures were determined by ELISA (OPT-EIA Set, Pharmingen). Mean concentrations of cytokines in 3 wells are shown. For ELISpot assays, fresh whole PBMCs (adherent cell-depleted) were incubated with various APC preparations for 14–18 hr in 96-well plates. Cultured cells were washed and transferred into an ELISpot assay kit (Pharmingen) with 96-well filtration plates coated with antihuman IFN-γ capture antibody for 3 hr. After wells were washed extensively with PBS, biotinylated antihuman IFN-γ antibody was added. Two hours later, spots were detected by avidin-biotin-peroxidase complex and aminoethyl carbazole solution. Mean values of the spots in 3 wells are shown.

Cr-release assay

The Cr-release assay was performed as described.[9] NKT-sensitive U937 lymphoma target cells were labeled with 100 μCi sodium chromate (Amersham, Little Chalfont, UK) for 1 hr. Cultured cells containing effector cytotoxic cells were seeded into 96-well round-bottomed plates at the indicated E: T ratios on the ^{51}Cr-labeled target cells (1 × 10^4). Percent specific ^{51}Cr release was calculated by the following formula: %specific lysis = (sample cpm − spontaneous cpm) × 100/(maximum cpm − spontaneous cpm). Spontaneous cpm was calculated from the supernatant of target cells alone, and maximum release was obtained by adding 1N HCl to target cell suspension. Data are expressed as mean values of triplicate cultures with SD.

Results

Expansion of Vα24$^+$ NKT cells by αGalCer-loaded IL-2/GM-CSF-cultured PBMCs

Whole PBMCs from HV1 or HV2 were cultured for 7 days in the presence of rhIL-2 (0–100 JRU/ml) and/or rhIL-4 (0–500 U/ml) with rhGM-CSF (800 U/ml), loaded with αGalCer (100ng/ml) or vehicle for the last 18 hr, irradiated and then used as stimulators. Freshly prepared autologous PBMCs (2 × 10^5, adherent cell-depleted) from the same volunteers were cocultured for 6 days in the presence of stimulator cells (1 × 10^5 or 4 × 10^4). Flow-cytometric analysis was performed to detect Vα24$^+$Vβ11$^+$ cells. Vα24$^+$ NKT cell expansions of more than 20-fold (in HV1) and 50-fold (in HV2) were detected when αGalCer-loaded PBMCs

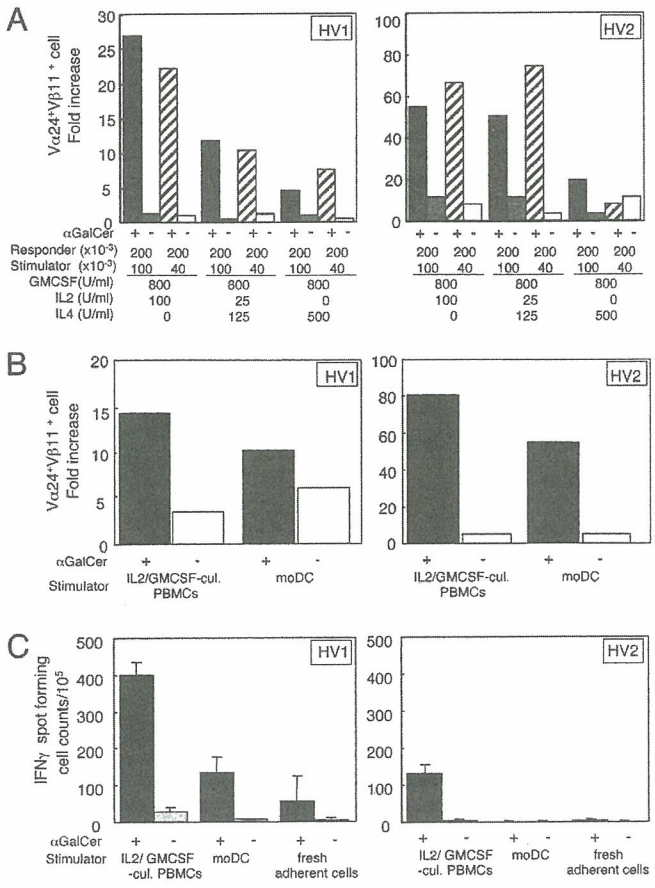

FIGURE 1 – Vα24$^+$ NKT cell expansion and IFN-γ production from αGalCer-loaded IL-2/GM-CSF-cultured PBMCs. (*a*) Whole PBMCs from HV1 or HV2 were cultured for 7 days in the presence of rhIL-2 (0–100 JRU/ml) and/or rhIL-4 (0–500 U/ml) with rhGM-CSF (800 U/ml), loaded with αGalCer (100 ng/ml) or vehicle for the last 18 hr, irradiated and then used as stimulators. Freshly prepared autologous PBMCs (2×10^5, adherent cell-depleted) from the same volunteers were cocultured for 6 days in the presence of stimulator cells (1×10^5 or 4×10^4) and 25 JRU/ml of IL-2. Flow-cytometric analysis was performed to detect Vα24$^+$Vβ11$^+$ cells. Three independent experiments were performed with similar results. (*b*) The efficiency of αGalCer-loaded IL-2/GM-CSF-cultured PBMCs (cultured in the presence of 100 JRU/ml of IL-2 and 800 U/ml of GM-CSF) at inducing Vα24$^+$ NKT cell expansion was compared to that of CD11c$^+$ moDCs. Freshly prepared autologous PBMCs (2×10^5, adherent cell-depleted) were cocultured for 6 days with stimulator cells (4×10^4) in the presence of 100 U/ml of IL-2. (*c*) The numbers of IFN-γ-producing cells upon stimulation with αGalCer-loaded IL-2/GM-CSF-cultured PBMCs were determined. Freshly prepared PBMCs (1×10^5) after depletion of adherent cells, CD8$^+$ cells and CD56$^+$ cells were cocultured for 15 hr with αGalCer-loaded IL-2/GM-CSF-cultured PBMCs (2×10^4), purified CD11c$^+$ moDCs (2×10^4) or fresh adherent cells (2×10^4). ELISpot assays were performed to detect IFN-γ-producing cells in cultures. Mean values with SDs are shown.

cultured with IL-2 (100 JRU/ml) and GM-CSF (800 U/ml) were used as stimulators (Fig. 1*a*). The magnitude of the expansion was decreased when PBMCs were cultured in the presence of IL-4 (125 U/ml and 500 U/ml for HV1, 500 U/ml for HV2). Next, the ability of αGalCer-loaded IL-2/GM-CSF-cultured PBMCs (PBMCs cultured in the presence of 100 JRU/ml of IL-2 and 800 U/ml of GM-CSF) to induce Vα24$^+$ NKT cell expansion was compared to that of CD11c$^+$ moDCs, prepared by cultivating adherent PBMC cells with IL-4 (500 U/ml) and GM-CSF (800 U/ml) for 7 days (Fig. 1*b*). For both HV1 and HV2, the expansion of Vα24$^+$ NKT cells induced by IL-2/GM-CSF-cultured PBMCs was comparable to that induced by purified CD11c$^+$

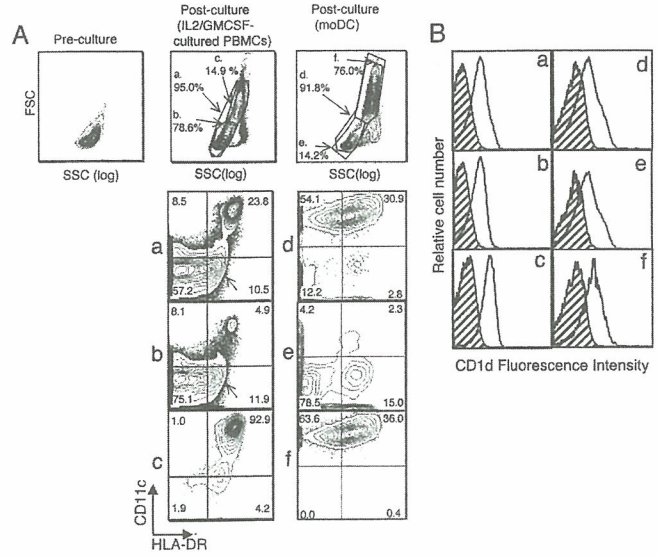

FIGURE 2 – HLA-DR/CD11c profiles and CD1d expression on several fractions of IL-2/GM-CSF-cultured PBMCs. (*a*) IL-2/GM-CSF-cultured PBMCs and moDCs prepared as described in the legend to Figure 1*b* were subjected to flow-cytometric analysis. SSC/FSC profiles of PBMCs before culture (Pre-culture) and after culture with IL-2 and GM-CSF (Post-culture) and with moDCs are shown in upper panels. Numbers represent the percent of cells present in each gate (a–f). Representative HLD-DR/CD11c profiles of cells of both small (SSC^{low}FSC^{low}) and large (SSC^{high}FSC^{high}) sizes (gates a and d), of cells of small size containing mostly lymphocytes (gates b and e) and of cells of large size containing mostly CD11c$^+$ cells (gates c and f) are shown. Arrows in (*a,b*) indicate substantial numbers of CD11c$^-$ cells expressing low levels of HLA-DR. The percentages of cells in each quadrant are also shown. (*b*) Representative CD1d profiles of the cells in each gate are shown with background staining with isotype-matched MAb (hatched areas).

moDCs. Concurrently, we assessed the number of IFN-γ-producing cells following stimulation with IL-2/GM-CSF-cultured PBMCs (Fig. 1*c*). Freshly prepared PBMCs (1×10^5) depleted of CD8$^+$ cells, CD56$^+$ cells and adherent cells were cocultured for 15 hr with αGalCer-loaded, IL-2/GM-CSF-cultured PBMCs or purified CD11c$^+$ moDCs. ELISpot assays were performed to detect IFN-γ-producing cells in the cultures. As shown in Figure 1*c*, the number of IFN-γ-producing cells in the culture with IL-2/GM-CSF-cultured PBMCs was significantly higher than that in the culture with CD11c$^+$ moDCs.

Characterization of IL-2/GM-CSF-cultured PBMCs

Next, IL-2/GM-CSF-cultured PBMCs and moDCs prepared as in Figure 1*b* were subjected to flow-cytometric analysis. Figure 2*a* shows SSC/FSC profiles of the cultured cells (upper) and representative HLD-DR/CD11c profiles of cells present in each gate (a–f): cells of both small and large size (gates a and d), cells of small size containing mostly lymphocytes (gates b and e) and cells of large size containing mostly CD11c$^+$ cells (gates c and f). IL-2/GM-CSF-cultured PBMCs included about 15% large and forward scatter cells (gate c) and >23% (23.8%) phenotypically typical DCs (HLA-DR$^+$ and CD11c$^+$, see HLA-DR/CD11c profile of gate a). Among moDCs, 76% were large and forward scatter cells (gate f). The small cells (gate b) in the IL-2/GM-CSF-cultured PBMCs included only a few (4.9%) HLA-DR$^+$ and CD11c$^+$ cells. Substantial numbers of CD11c$^-$ cells among IL-2/GM-CSF-cultured PBMCs expressed low but significant levels of HLA-DR (arrows in gates a and b); however, most large cells (gate c) in IL-2/GM-CSF-cultured PBMCs (>90%) expressed high levels of HLA-DR and CD11c. In contrast, almost 100% of the large cells (gate f) in moDCs expressed high levels of CD11c, but expression

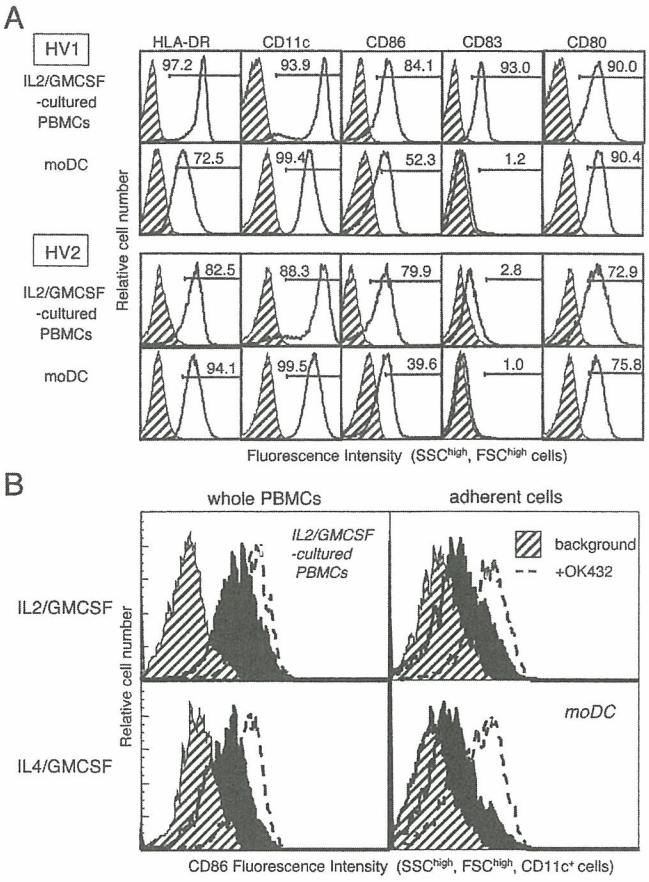

FIGURE 3 – Cell surface expression of CD86, CD83 and CD80 on a $SSC^{high}FSC^{high}$ DC fraction of IL-2/GM-CSF-cultured PBMCs. (*a*) Representative profiles of the expression of various cell surface marker antigens (HLA-DR, CD11c, CD86, CD83 and CD80) on $SSC^{high}FSC^{high}$ cells in IL-2/GM-CSF-cultured PBMCs or moDCs from HV1 and HV2 are shown with background staining (hatched areas). Numbers represent the percent of cells within the indicated gate. (*b*) Whole PBMCs (left panels) or adherent cells (right panels) were cultured for 7 days in the presence of IL-2 and GM-CSF (upper panels) or IL-4 and GM-CSF (lower panels). Maturation of DCs was induced by stimulation with OK432 (0.1 KE/ml) for 24 hr. Flow-cytometric analysis was performed to detect CD86 expression on $SSC^{high}FSC^{high}CD11c^{+}$ cells in culture. CD86 profiles with (dashed lines) or without (filled area) OK432 stimulation are shown, with background staining profiles (hatched areas).

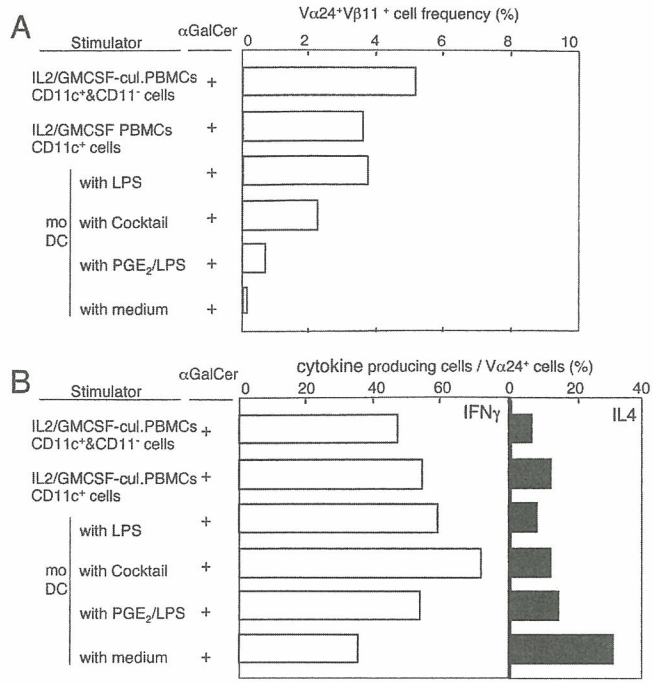

FIGURE 4 – Expansion of IFN-γ/IL-4 production by $V\alpha24^{+}$ NKT cells with IL-2/GM-CSF-cultured PBMCs. (*a*) The ability of whole IL-2/GM-CSF-cultured PBMCs to expand $V\alpha24^{+}$ NKT cells and their production of cytokines (IL-4 and IFN-γ) were compared to a $CD11c^{+}$ fraction of IL-2/GM-CSF-cultured PBMCs and moDCs with or without further stimulation by LPS, a cytokine cocktail (IL-1β, TNFα and PGE_2) or PGE_2/LPS for 2 days. After pulsing with αGalCer for 18 hr and subsequent irradiation, stimulator cells were cocultured with adherent cell-depleted fresh PBMCs. On day 6, flow-cytometric analysis was performed to detect $V\alpha24^{+}V\beta11^{+}$ cells. The percentages of $V\alpha24^{+}V\beta11^{+}$ cells among live cells are shown. (*b*) Cytoplasmic cytokine staining with anti-IL-4 and anti-IFN-γ in conjunction with cell surface staining with anti-Vα24 and anti-Vβ11 MAbs. The percentages of IFN-γ- or IL-4-producing cells among $V\alpha24^{+}V\beta11^{+}$ cells are shown.

of HLA-DR was more heterogenous, with only 36% of high HLA-DR-expressing cells. Concurrently, we determined the expression of CD1d antigen-presenting molecules of αGalCer for $V\alpha24^{+}$ NKT cells. Representative CD1d profiles of the cells present in each gate are shown in Figure 2*b*. In both IL-2/GM-CSF-cultured PBMCs and moDCs, the majority of the cells, regardless of their FSC or SSC, expressed similar levels of CD1d.

Cell surface expression of CD86, CD83 and CD80 on IL-2/GM-CSF-cultured PBMCs

In addition, we assessed the expression of other cell surface marker antigens (CD86, CD83 and CD80) on $SSC^{high}FSC^{high}$ cells in IL-2/GM-CSF-cultured PBMCs and moDCs from HV1 and HV2. In both HV1 and HV2, $SSC^{high}FSC^{high}$ cells in IL-2/GM-CSF-cultured PBMCs expressed substantial levels of CD86, CD83 and CD80 but those in moDCs expressed only CD86 and CD80 (Fig. 3*a*).

Next, whole PBMCs or adherent cells were cultured for 7 days in the presence of IL-2 and GM-CSF or IL-4 and GM-CSF, and the maturation of DCs was induced by stimulation with OK432 for 24 hr. As shown in Figure 3*b*, expression levels of CD86 on $SSC^{high}FSC^{high}CD11c^{+}$ cells in IL-2/GM-CSF-cultured PBMCs (upper left) were significantly higher than those in IL-4/GM-CSF-cultured PBMCs (lower left) or immature moDCs (lower right) (compare filled areas in Fig. 3*b*). Expression of CD86 was significantly higher in whole PBMC cultures than in cultures of purified adherent cells stimulated with IL-2 and GM-CSF (compare profiles upper left and right). In all 4 $CD11c^{+}$ cell preparations, levels of CD86 were increased and were similar when the cells were stimulated with OK432 (compare dashed lines in Fig. 3*b*). These results suggest that $CD11c^{+}$ cells in IL-2/GM-CSF-cultured PBMCs express high levels of CD86 and are in a relatively more mature state, while $CD11c^{+}$ cells in moDCs need to be stimulated to become mature.

IL-2/GM-CSF-cultured PBMCs induce efficient expansion of $V\alpha24^{+}$ NKT cells that produce IFN-γ preferentially

We then tested the ability of whole IL-2/GM-CSF-cultured PBMCs to expand $V\alpha24^{+}$ NKT cells and examined their production of cytokines (IL-4 and IFN-γ) in the absence of IL-2 in cultured medium compared to the $CD11c^{+}$ fraction of IL-2/GM-CSF-cultured PBMCs and moDCs with or without further stimulation by LPS (1,000 ng/ml) and a cytokine cocktail (IL-1β, 10 ng/ml; TNF-α, 10 ng/ml; and PGE_2, 1 μg/ml) for 2 days[30] or PGE_2 (5 μg/ml) plus LPS (100 ng/ml). As shown in Figure 4*a*, the

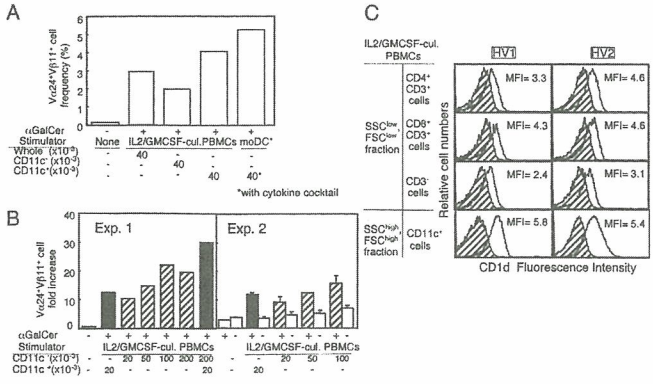

FIGURE 5 – CD11c$^-$ cells in IL-2/GM-CSF-cultured PBMCs induce expansion of Vα24$^+$Vβ11$^+$ NKT cells. (*a*) Whole IL-2/GM-CSF-cultured PBMCs, the CD11c$^+$ and CD11c$^-$ fractions of IL-2/GM-CSF-cultured PBMCs were prepared and their abilities to expand Vα24$^+$ NKT cells were compared. As a positive control, mature moDCs induced with a cytokine cocktail (IL-1β, TNFα and PGE_2) were included. The frequencies of Vα24$^+$Vβ11$^+$ cells are shown. (*b*) Fresh PBMCs (2×10^5, adherent cell-depleted) were cultured with IL-2 for 6 days in the presence or absence of irradiated αGalCer-loaded CD11c$^+$ cells (2×10^4) or titrated doses of CD11c$^-$ cells (shown in Exp. 1). αGalCer-pulsed and nonpulsed cells were used in Exp. 2. (*c*) Levels of CD1d expression on CD4$^+$CD3$^+$, CD8$^+$CD3$^+$ and CD3$^-$ cells in CD11c$^-$ lymphocyte fractions (SSC^{low}FSC^{low}CD11c$^-$) in IL-2/GM-CSF-cultured PBMCs and CD11c$^+$ cells in the SSC^{high}FSC^{high} gate are shown. MFI shown in each panel.

frequency of Vα24$^+$Vβ11$^+$ Vα24 NKT cells was highest in cultures with whole IL-2/GM-CSF-cultured PBMCs. Slightly lower but substantial levels (approx. 4%) of Vα24NKT cells were induced in the culture with CD11c$^+$ IL-2/GM-CSF-cultured PBMCs and moDCs after 2-day stimulation with LPS (second and third groups in Fig. 4*a*). Essentially no expansion was induced by nonstimulated immature moDCs (bottom group in Fig. 4*a*).

To assess the production of cytokines by expanded Vα24$^+$ cells, we performed cytoplasmic cytokine staining with anti-IL-4 and anti-IFN-γ in conjunction with cell surface staining with anti-Vα24 (Fig. 4*b*). Most of the APCs prepared as indicated induced substantial levels of IFN-γ-producing Vα24$^+$ cells. Immature moDCs (with medium) showed the lowest ability to induce IFN-γ-producing Vα24$^+$ cells. Interestingly, IL-2/GM-CSF-cultured PBMCs induced very low levels (<10%) of IL-4-producing Vα24$^+$ cells in culture compared to the other preparations (Fig. 4*b*, top group). It is of interest that immature moDCs induced the highest frequency of IL-4-producing Vα24$^+$ cells (>30%). These results suggest that IL-2/GM-CSF-cultured PBMCs possess a potent ability to expand Vα24$^+$ cells that produce substantial levels of IFN-γ and small amounts of IL-4.

CD11c$^-$ cells in IL-2/GM-CSF-cultured PBMCs induce expansion of Vα24$^+$Vβ11$^+$ NKT cells

In addition to DCs and macrophages, human activated T cells express CD1d molecules.[28–30] Therefore, we studied whether CD11c$^-$ cells themselves induced αGalCer-dependent expansion of Vα24$^+$ NKT cells. We prepared CD11c$^+$ and CD11c$^-$ populations from whole IL-2/GM-CSF-cultured PBMCs and compared their abilities to expand Vα24$^+$ NKT cells (Fig. 5*a*). Whole IL-2/GM-CSF-cultured PBMCs, the CD11c$^+$ and CD11c$^-$ fractions of whole IL-2/GM-CSF-cultured PBMCs and mature CD11c$^+$ moDCs stimulated with a cytokine cocktail were pulsed with αGalCer and used as stimulators. Nonadherent fresh PBMCs (2×10^5, adherent cell-depleted) were cultured with stimulators for 6 days in the presence of IL-2. Although levels of Vα24$^+$ NKT cell expansion by CD11c$^-$ populations (approx. 2%) were slightly less than those of whole (approx. 3%) or the CD11c$^+$ fraction (approx. 4%) of IL-2/GM-CSF-cultured PBMCs, certain levels of expansion were consistently observed. Next, adherent cell-depleted PBMC responders were cocultured with titrated doses of CD11c$^-$ cell stimulator cells. As shown in Figure 5*b*, experiment 1 (Exp. 1), levels of Vα24$^+$ NKT cell expansion produced by 20×10^3 CD11c$^-$ cells were slightly lower than those produced by 20×10^3 CD11c$^+$ cells, while levels became higher when 50×10^3, 100×10^3 and 200×10^3 CD11c$^-$ cells were used. We included αGalCer-nonpulsed cells in Exp. 2 to demonstrate αGalCer dependence in the expansion of Vα24$^+$ NKT cells. Next, levels of CD1d expression on CD4$^+$CD3$^+$, CD8$^+$CD3$^+$ and CD3$^-$ cells in the CD11c$^-$ lymphocyte fraction (SSC^{low}-FSC^{low}CD11c$^-$) of IL-2/GM-CSF-cultured PBMCs were compared to those on SSC^{high}FSC^{high}CD11c$^+$ cells in HV1 and HV2 (Fig. 5*c*). Although the levels were slightly lower, CD4$^+$CD3$^+$, CD8$^+$CD3$^+$ and CD3$^-$ lymphocytes expressed certain levels of CD1d on their cell surface. These results suggest that CD11c$^-$ cells in IL-2/GM-CSF-cultured PBMCs possess some level of αGalCer antigen-presenting ability to expand Vα24$^+$ NKT cells.

Ability to expand Vα24$^+$Vβ11$^+$ cells in moDCs is enhanced by cocultivation with CD11c$^-$ cells in whole IL-2/GM-CSF-cultured PBMCs

Since CD11c$^+$ cells in IL-2/GM-CSF-cultured PBMCs showed potent activity in Vα24 NKT cell expansion at levels comparable to mature moDCs induced by LPS stimulation (Fig. 4*a*), we next assessed whether CD11c$^-$ cells in IL-2/GN-CSF-cultured PBMCs induced maturation of DCs. CD11c$^+$ moDCs were stimulated with LPS, cytokine cocktail (IL-1β, TNF-α and PGE_2) or irradiated CD11c$^-$ cells derived from IL-2/GM-CSF-cultured PBMCs for 1–3 days. Stimulated CD11c$^+$ moDCs were irradiated and cocultured with nonadherent fresh PBMCs (2×10^5, adherent cell-depleted) containing Vα24$^+$ NKT cells in the presence of IL-2 for 6 days. Numbers of Vα24$^+$Vβ11$^+$ cells in the cultures were assessed by flow cytometry. Data are shown as Vα24$^+$Vβ11$^+$ frequency and fold increase in Figure 6*a* and *b*, respectively. By either indicator, when irradiated CD11c$^-$ cells in IL-2/GM-CSF-cultured PBMCs were used as stimulators for moDC maturation for 3 days, levels of expansion of Vα24$^+$Vβ11$^+$ cells were equivalent to those in LPS- or cytokine cocktail–stimulated moDCs. One day was enough for LPS or the cytokine cocktail to induce maturation of moDCs, but 3 days were needed for the CD11c$^-$ cells to give moDCs the ability to expand NKT cells.

To further examine whether CD11c$^-$ cells induced maturation of CD11c$^+$ cells, CD11c$^+$ moDCs were stimulated with various doses of irradiated CD11c$^-$ cells derived from IL-2/GM-CSF-cultured PBMCs for 3 days, and then expression of CD86 on CD11c$^+$ cells was assessed. Figure 6*c* shows a representative result of MFI of CD86 staining on moDCs. As expected, a CD11c$^-$ cell dosage-dependent increase in the MFI of CD86 staining on moDCs was detected. Moreover, to identify functional effector molecules that are produced by CD11c$^-$ cells and induce DC maturation, various MAbs (5 μg/ml) were added to the culture with CD11c$^+$ moDCs and irradiated CD11c$^-$, and then the cell surface expression of CD86 on CD11c$^+$ moDCs was assessed (Fig. 6*d*). Among MAbs tested, anti-TNF-α MAb substantially inhibited the induction of CD86 on moDCs. No apparent effects were seen in the groups with MAb specific for other cytokines, including INF-γ, IL-4 and IL-12. These results suggest that CD11c$^-$ cells in IL-2/GM-CSF-cultured PBMCs are able to support the maturation of CD11c$^+$ moDCs to induce the expansion of Vα24$^+$ NKT cells and that TNF-α plays important roles in the CD11c$^-$ cell–mediated maturation of CD11c$^+$ moDCs.

CD11c$^-$ CD3$^+$ T cells produce substantial amounts of TNF-α and are involved in the maturation of DCs

To investigate further which subpopulations of CD11c$^-$ cells in IL-2/GM-CSF-cultured PBMCs are involved in moDC maturation, we depleted the PBMC cultures of CD11c$^-$CD56$^+$ cells,

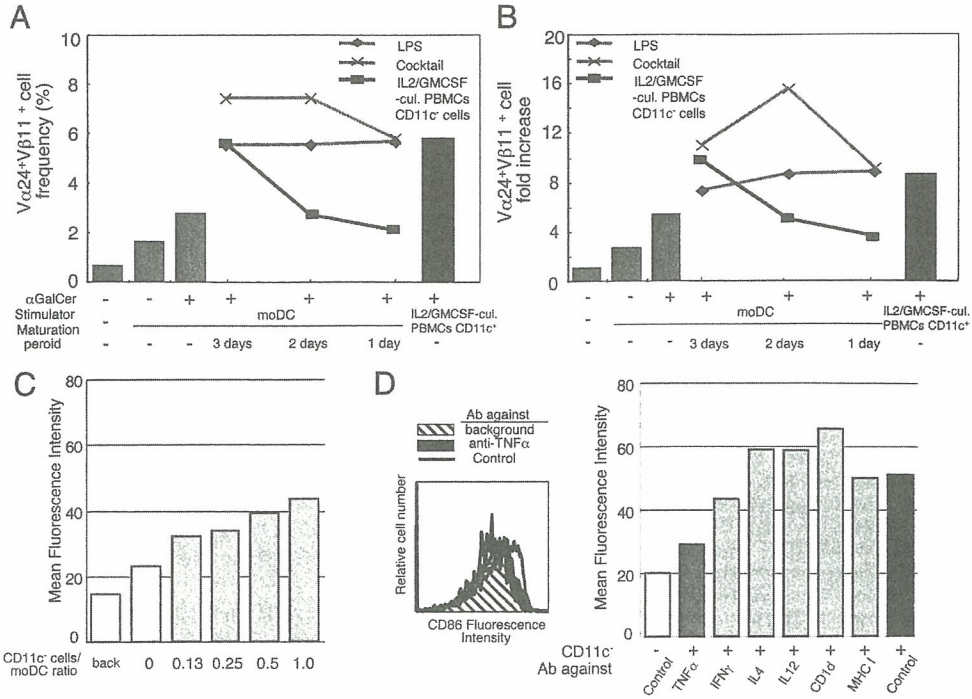

FIGURE 6 – The ability of moDCs to expand $V\alpha24^+V\beta11^+$ cells is enhanced by cocultivation with $CD11c^-$ cells in whole IL-2/GM-CSF-cultured PBMCs. (*a,b*) $CD11c^+$ moDCs (4×10^4) were stimulated with LPS or a cytokine cocktail (IL-1β, TNFα and PGE_2) or with irradiated $CD11c^-$ cells (2×10^4) derived from IL-2/GM-CSF-cultured PBMCs for 1–3 days. Nonadherent fresh PBMCs (2×10^5, adherent cell-depleted) were cultured with stimulators for 6 days in the presence of IL-2. $CD11c^+$ cells in IL-2/GM-CSF-cultured PBMCs were included as a control. Numbers of $V\alpha24^+V\beta11^+$ cells in cultures were assessed by flow cytometry. Data are shown as $V\alpha24^+V\beta11^+$ frequency (*a*) and fold increase (*b*). (*c*) $CD11c^+$ moDCs (2×10^5) were cocultured with several doses of irradiated $CD11c^-$ cells derived from IL-2/GM-CSF-cultured PBMCs for 3 days. Flow-cytometric analysis was performed to detect CD86 expression on $SSC^{high}FSC^{high}CD11c^+$ cells in culture. Representative MFIs of CD86 staining on moDCs are shown. Background represents background MFI with isotype-matched MAb. (*d*) $CD11c^+$ moDCs (2×10^5) were cultured with irradiated $CD11c^-$ cells (1×10^5) in the presence of 5 μg/ml of indicated MAbs for neutralization. Left panel shows a representative CD86 staining profile of moDCs in the presence of anti-IgG1 (line) or anti-TNFα (filled area) with background staining (hatched area). Right panel shows representative MFIs of CD86 staining on moDCs stimulated with $CD11c^-$ cells in the presence of a MAb specific for the indicated molecules. Control, isotype-matched control antibody.

$CD11c^-CD3^+$ cells or both $CD11c^-CD56^+$ and $CD11c^-CD3^+$ cells prior to IL-2/GM-CSF cultivation and tested the ability of the cultures to induce CD86 molecules on moDCs. As shown in Figure 7*a*, upregulation of CD86 was not affected by the depletion of $CD56^+$ cells but was substantially inhibited by the depletion of $CD3^+$ cells. The depletion of both $CD56^+$ cells and $CD3^+$ cells resulted in almost no induction of CD86 on moDCs. These results suggest that $CD3^+$ T cells in PBMCs are important for the maturation of moDCs and that $CD56^+$ NK cells may play some role in the maturation process. Next, we isolated $CD11c^-CD3^+$ cells, $CD11c^-CD3^-CD56^+$ cells and $CD3^-CD56^-$ cells from IL-2/GM-CSF-cultured PBMCs and assessed their production of TNF-α. A substantial amount of TNF-α was secreted from $CD3^+$ cells. Levels of TNF-α were approximately 1/5 and 1/3 in the $CD3^-CD56^+$ and $CD3^-CD56^-$ cell cultures, respectively (Fig. 7*b*). These results suggest that $CD3^+$ T cells in IL-2/GM-CSF-cultured PBMCs are the major producer of TNF-α. Next, to examine the requirement for IL-2 in PBMC culture for the induction of CD86 on DCs, PBMCs were cultured with GM-CSF alone, IL-2 alone or IL-2 and GM-CSF and CD86 expression on SSC^{high}-FSC^{high} cells (DC) and CD69 expression on $CD3^+$ cells (T cells) assessed (Fig. 7*c*). Cultivation with GM-CSF alone generated 56.4% of $CD11c^+$ cells, but CD86 molecules were not induced significantly on DCs (MFI = 16). Cultivation with IL-2 alone induced CD86 molecules on DCs (MFI = 58) but generated only 5.0% of $CD11c^+$ cells. Cultivation with both IL-2 and GM-CSF generated 15.3% of $CD11c^+$ cells with sufficient CD86 induction (MFI = 61). More than 30% of T cells were activated to express CD69 in cultures containing IL-2. These results indicate that IL-2 is required for the maturation of DCs and that GM-CSF is important for the generation of $CD11c^+$ cells. Thus, it is most likely that TNF-α is produced by $CD11c^-$ T cells upon activation with IL-2 and then TNF-α induces the maturation of DCs generated by GM-CSF in PBMC culture.

Cytotoxic activity of $V\alpha24^+$ NKT cells stimulated with αGalCer-loaded IL-2/GM-CSF-cultured PBMCs

We assessed whether $V\alpha24^+$ NKT cells activated with αGalCer-loaded IL-2/GM-CSF-cultured PBMCs show cytotoxic activity against U937 cells (Fig. 8). Freshly prepared PBMCs from HV1 were cultured with αGalCer-loaded IL-2/GM-CSF-cultured PBMCs for 7 days, activated $V\alpha24^+$ cells were purified with MACS and their cytotoxic activity on U937 cells was examined with a standard Cr-release assay. Significantly increased cytotoxic activity against NKT cell-sensitive U937 target cells was induced by $V\alpha24^+$ NKT cells activated with αGalCer-loaded IL-2/GM-CSF-cultured PBMCs compared to those with αGalCer-unloaded IL-2/GM-CSF-cultured PBMCs or $V\alpha24^-$ cells containing activated T cells.

Induction of cytokine production and proliferation of in vitro activated $V\alpha24^+$ NKT cells by $CD11c^+$ and $CD11c^-$ cells in IL-2/GM-CSF-cultured PBMCs

Finally, we examined whether $CD11c^+$ and $CD11c^-$ cells exert significant activity to expand *in vitro* activated $V\alpha24^+$ NKT cells. PBMCs from HV1 were cultured with IL-2 and αGalCer for 7 days, and the $V\alpha24^-$positive cells were enriched using a MACS

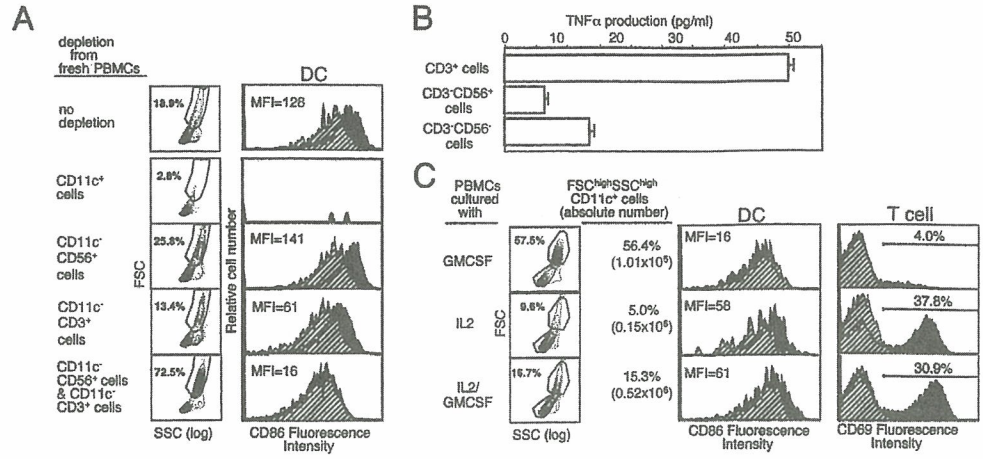

FIGURE 7 – CD11c$^-$ CD3$^+$ T cells produce substantial amounts of TNFα and play a critical role in the maturation of DCs. (*a*) CD11c$^+$ cells, CD11c$^-$CD56$^+$ cells, CD11c$^-$CD3$^+$ cells or CD11c$^-$CD56$^+$ plus CD11c$^-$CD3$^+$ cells were depleted from freshly prepared PBMCs. Undepleted whole PBMCs and various cell population-depleted PBMCs were cultured for 7 days in the presence of IL-2 (100 JRU/ml) and GM-CSF (800 U/ml). Flow-cytometric analysis was performed to assess the expression of CD86 on SSC^{high}FSC^{high}CD11c$^+$ cells in the cultures. Representative profiles of CD86 staining on SSC^{high}FSC^{high}CD11c$^+$ cells with MFIs are shown. (*b*) CD3$^+$ cells, CD3$^-$ CD56$^+$ cells and CD3$^-$CD56$^-$ cells in IL-2/GM-CSF-cultured PBMCs were isolated and cultured in 200 μl culture medium for 24 hr. Mean concentrations of TNFα in culture supernatants are shown with SDs. (*c*) Whole PBMCs were cultured for 7 days in the presence of GM-CSF (800 U/ml), IL-2 (100 JRU/ml) or IL-2/GM-CSF (IL-2 100 JRU/ml, GM-CSF 800 U/ml). Flow-cytometric analysis was performed to assess the expression of CD86 on SSC^{high}FSC^{high}CD11c$^+$ cells (DC) and CD69 expression on SSC^{low}FSC^{low}CD3$^+$ cells (T cells) in the cultures. The percentages and absolute numbers of SSC^{high}FSC^{high}CD11c$^+$ cells in the culture are also shown.

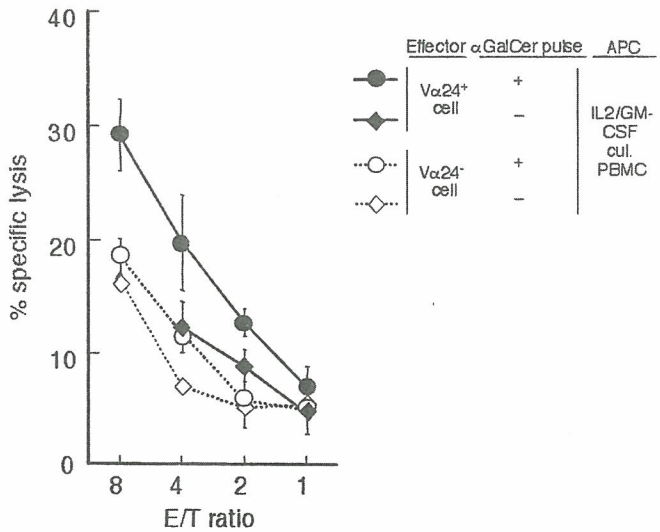

FIGURE 8 – Cytotoxic activity of Vα24$^+$ NKT cells stimulated with αGalCer-loaded IL-2/GM-CSF-cultured PBMCs. Irradiated αGalCer-loaded (or unloaded) IL-2/GM-CSF-cultured PBMCs (1×10^5) were cocultured with adherent cell-depleted fresh PBMCs (2×10^5) containing Vα24$^+$ NKT cells for 7 days in the presence of IL-2. Activated Vα24$^+$ cells were separated from cultured cells by MACS sorting. Vα24$^-$ cells were prepared by depletion of Vα24$^+$ cells, CD16$^+$ cells and CD56$^+$ cells. Vα24$^+$ cells and Vα24$^-$ cells were seeded with ^{51}Cr-labeled NKT cell-sensitive U937 target cells. Percent specific ^{51}Cr release was calculated as described in Material and methods.

separation column. Enriched Vα24$^+$ NKT cells were subjected to another 7-day stimulation with IL-2 and αGalCer-loaded irradiated fresh PBMCs from HV1. More than 96% of the cells were Vα24$^+$Vβ11$^+$ cells (Fig. 9*a*). Activated Vα24$^+$ NKT cells were cocultured with irradiated αGalCer-loaded immature moDCs, CD11c$^+$ cells or CD11c$^-$ cells prepared from IL-2/GM-CSF-cultured PBMCs. The proliferative responses (Fig. 9*b*) and production of IFN-γ and IL-4 (Fig. 9*c*) from *in vitro* activated Vα24$^+$ NKT cells were examined. Proliferative responses of Vα24$^+$ NKT cells were induced by immature moDCs, CD11c$^+$ cells and CD11c$^-$ cells in IL-2/GM-CSF-cultured PBMCs; and levels were highest in immature moDCs. All these responses were significantly inhibited by the presence of an anti-CD1d MAb but not a control anti-MHC class I MAb, suggesting that the proliferation is dependent on CD1d. As can be seen in Figure 9*c*, CD11c$^+$ cells induced substantial levels of both IFN-γ and IL-4 production in activated Vα24$^+$ NKT cells. Although levels were low, CD11c$^-$ cells also induced IFN-γ and IL-4 production in a cell dose-dependent manner. These results suggest that, although levels are lower, both CD11c$^+$ and CD11c$^-$ cells in IL-2/GM-CSF-cultured PBMCs are able to stimulate *in vitro* activated Vα24$^+$ NKT cells in a CD1d-dependent manner.

Discussion

Here, we demonstrate that IL-2/GM-CSF-cultured PBMCs are able to expand freshly prepared autologous Vα24$^+$ NKT cells very effectively and induce their ability to produce large amounts of IFN-γ and exert significant cytotoxicity to tumor target cells. Especially, CD11c$^+$ cells in IL-2/GM-CSF-cultured PBMCs expressed high levels of CD86 (Fig. 3*b*), suggesting that these cells were in a relatively more mature state and induced efficient expansion of Vα24$^+$ NKT cells and preferential production of IFN-γ at levels equivalent to those of mature moDCs (Fig. 4*a,b*). Maturation of CD11c$^+$ cells in IL-2/GM-CSF-cultured PBMCs was induced by CD11c$^-$ cells present in culture (Fig. 6*a–c*). TNF-α appeared to play important roles in the maturation of CD11c$^+$ cells. In addition, although levels were slightly lower, even CD11c$^-$ cells expressed CD1d and showed substantial stimulatory activity on freshly prepared Vα24$^+$ NKT cells, resulting in expansion and IFN-γ production (Fig. 5). Thus, IL-2/GM-CSF-cultured PBMCs can be used as potent APCs for αGalCer presentation to naive Vα24$^+$ NKT cells.

The maturation of CD11c$^+$ DCs is well established by cultivation of moDCs with TNF-α alone or a cytokine cocktail including TNF-α, IL1β, PGE_2 with or without IL-6[32] as well as other material such as LPS and CD40-L.[27] However, maturation also appears to occur through cell–cell contact, such as with lymphokine-activated lymphocytes or activated NK cells.[33] In particular, it has

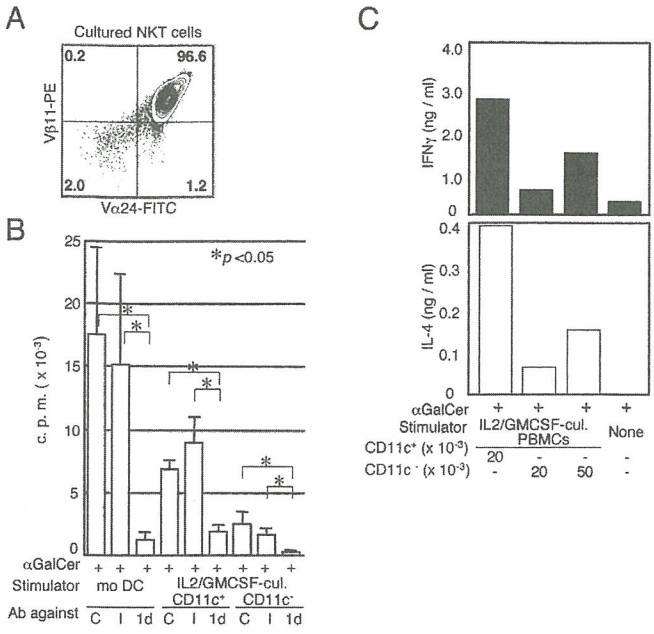

FIGURE 9 – Induction of cytokine production and proliferation of *in vitro* activated Vα24$^+$ NKT cells by CD11c$^+$ and CD11c$^-$ cells in IL-2/GM-CSF-cultured PBMCs. CD11c$^+$ and CD11c$^-$ fractions from IL-2/GM-CSF-cultured PBMCs were prepared, and their ability to induce cytokine production by Vα24$^+$ NKT cells was compared. (*a*) Vα24/Vβ11 profiles of *in vitro* activated Vα24$^+$ NKT cells prepared by 2 cycles of cultivation with IL-2 and αGalCer for 7 days. The percentages of cells present in each quadrant are also shown. (*b*) Mean ^{3}H uptakes of activated Vα24$^+$ NKT cells in triplicate cultures are shown with SDs. Anti-CD1d MAb (1d, 10 μg/ml), anti-MHC class I MAb (I, 10 μg/ml) and control isotype-matched antibody (C) were added to the culture. *$p < 0.05$. (*c*) *In vitro* activated Vα24$^+$ NKT cells were cocultured with irradiated αGalCer-loaded CD11c$^+$ or CD11c$^-$ cells for 2 days. Concentrations of IFN-γ and IL-4 in the culture supernatant are shown.

been reported that NK cells can induce maturation of DCs *via* cell–cell interactions of MHC and NK receptors, as well as secreted cytokines such as IFN-γ and TNF-α.[34] In our study, phenotypic maturation of moDCs indeed occurred after cocultivation with CD11c$^-$ cells in IL-2/GM-CSF-cultured PBMCs (Fig. 6*c*). Moreover, we demonstrate that TNF-α is a critical cytokine for the maturation of moDCs by CD11c$^-$ cells (Fig. 6*d*). In the CD11c$^-$ fraction of IL-2/GM-CSF-cultured PBMCs, CD11c$^-$CD3$^+$ T cells appeared to play important roles in DC maturation (Fig. 7*a*). In addition, TNF-α was preferentially produced by CD11c$^-$CD3$^+$ T cells (Fig. 7*b*). Thus, the maturation of DCs induced by CD11c$^-$ T cells through TNF-α production appears to be critical for the efficient expansion and activation of Vα24$^+$ NKT cells to produce IFN-γ preferentially.

In DC therapy with HLA-ABC-restricted antigens, several preclinical investigations and clinical trials using *ex vivo* generated moDCs succeeded in producing tumor regression in patients with limited malignant tumors.[27,35,36] Mature DCs are much more effective at activating naive T cells and inducing antigen-specific T-cell responses.[37,38] As for Vα24$^+$ NKT cells, mature moDCs pulsed with αGalCer appear to have a better ability to induce Vα24$^+$ NKT cell expansion than either immature moDCs or monocytes.[32] Here, we show that the expansion of Vα24$^+$ NKT cells induced by naturally matured CD11c$^+$ DCs in IL-2/GM-CSF-cultured PBMCs was comparable to that induced by mature CD11c$^+$ moDCs stimulated additionally with LPS or cytokine cocktail.

Another interesting observation is that CD11c$^-$ cells in IL-2/GM-CSF-cultured PBMCs imparted a certain stimulatory activity to Vα24$^+$ NKT cells. CD11c$^-$ cells were shown to express CD1d (Fig. 2), and the majority (>75%) were T cells (data not shown). CD1d expression has been reported to be inducible on human T cells upon activation.[28–30] However, it has not been clarified whether activated CD1d-expressing T cells can successfully present αGalCer to human Vα24$^+$ NKT cells. We characterized CD11c$^-$ cells in IL-2/GM-CSF-cultured PBMCs very carefully to determine their ability to present αGalCer to human Vα24$^+$ NKT cells, causing them to proliferate and produce cytokines (Fig. 5), and concluded that CD11c$^-$ cells induced activation and expansion of Vα24$^+$ NKT cells, particularly freshly prepared Vα24$^+$ NKT cells.

There are many reports in the literature about the function of DCs in the regulation of T cell–mediated immune responses. The nature of the regulation has become more complicated due to the discovery of activation status and ontogenetically diverse subtypes of DC in murine models,[27,37] as well as the results of *in vitro* studies using human PBMCs. For instance, DCs cultured under some conditions, including the presence of IL-10, TGF-β, or steroids and at low DC/T cell ratios, induce naive CD4 T cells to differentiate into Th2 cells.[39,40] However, it is not known how the balance of Th1/Th2 cytokine production in Vα24$^+$ NKT cells is regulated by human αGalCer-loaded APCs. Here, we examined the Th1/Th2 cytokine profiles of Vα24$^+$ NKT cells activated by various αGalCer-loaded APCs and found that whole IL-2/GM-CSF-cultured PBMCs and CD11c$^+$ cells in IL-2/GM-CSF-cultured PBMCs induced preferential IFN-γ production in Vα24$^+$ NKT cells. The preferential IFN-γ production was superior or equal to that of mature moDCs. Moreover, the separation process of nonadherent cells is not required for the preparation of IL-2/GM-CSF-cultured PBMCs. In addition, there is no loss in cell number during preparation. Thus, IL-2/GM-CSF-cultured PBMCs represent an alternative potent material for tumor immunotherapy aimed at the *in vivo* activation and expansion of Vα24$^+$ NKT cells.

It has been reported that the number and/or function of Vα24$^+$ NKT cells in PBMCs from patients with malignant tumors is decreased compared to PBMCs from healthy volunteers and the amount of the decrease appears to be dependent on tumor type and clinical stage.[13,41–44] We reported that the number of Vα24$^+$ NKT cells among PBMCs is reduced in patients with lung cancer but their ability to produce IFN-γ remains intact.[13] In patients with advanced gastrointestinal cancers, the *in vitro* expansion of Vα24$^+$ NKT cells was impaired, although it recovered partially by coculture with G-CSF.[44] In patients with progressive malignant multiple myelomas, freshly prepared Vα24$^+$ NKT cells did not produce IFN-γ even after stimulation with αGalCer-loaded moDCs, although the dysfunction was considered to be reversible because functional Vα24$^+$ NKT cells could be expanded after *in vitro* culture.[41] Thus, it is speculated that αGalCer-loaded APC therapy will be useful for treating patients with early-stage malignancies who show no severe dysfunction of their Vα24$^+$ NKT cells; patients with advanced cancers may need to receive additional supportive therapy, such as adoptive administration of functional Vα24$^+$ NKT cells, prior to αGalCer-loaded APC therapy.

In summary, our results indicate that maturation of DCs induced by CD11c$^-$ T cells through TNF-α production appears to be critical for the efficient activation of Vα24$^+$ NKT cells by αGalCer to produce IFN-γ preferentially. In addition, activated Vα24$^+$ NKT cells with IL-2/GM-CSF-cultured PBMCs showed significant cytotoxic activity against tumor cells *in vitro*. Thus, use of IL-2/GM-CSF-cultured PBMCs is appropriate for tumor immunotherapy aimed at Vα24$^+$ NKT cell activation and expansion.

Acknowledgements

We thank Kirin Brewery for providing clinical grade αGalCer (KRN7000) for these studies and Ms. K. Sugaya and Ms. A. Nitta for excellent technical assistance.

References

1. Bendelac A, Rivera MN, Park SH, Roark JH. Mouse CD1-specific NK1 T cells: development, specificity, and function. Annu Rev Immunol 1997;15:535–62.
2. Taniguchi M, Nakayama T. Recognition and function of Vα14 NKT cells. Semin Immunol 2000;12:543–50.
3. Matsuda JL, Kronenberg M. Presentation of self and microbial lipids by CD1 molecules. Curr Opin Immunol 2001;13:19–25.
4. Taniguchi M, Harada M, Kojo S, Nakayama T, Wakao H. The regulatory role of Vα14 NKT cells in innate and acquired immune response. Annu Rev Immunol 2003;21:483–513.
5. Godfrey DI, MacDonald HR, Kronenberg M, Smyth MJ, Van Kaer L. NKT cells: what's in a name? Nature Rev Immunol 2004;4:231–7.
6. Smyth MJ, Godfrey DI, Trapani JA. A fresh look at tumor immunosurveillance and immunotherapy. Nat Immunol 2001;2:293–9.
7. Wilson SB, Delovitch TL. Janus-like role of regulatory iNKT cells in autoimmune disease and tumour immunity. Nature Rev Immunol 2003;3:211–22.
8. Porcelli SA, Modlin RL. The CD1 system: antigen-presenting molecules for T cell recognition of lipids and glycolipids. Annu Rev Immunol 1999;17:297–329.
9. Kawano T, Nakayama T, Kamada N, Kaneko Y, Harada M, Ogura N, Akutsu Y, Motohashi S, Iizasa T, Endo H, Fujisawa T, Shinkai H, et al. Antitumor cytotoxicity mediated by ligand-activated human Vα24 NKT cells. Cancer Res 1999;59:5102–5.
10. Brossay L, Chioda M, Burdin N, Koezuka Y, Casorati G, Dellabona P, Kronenberg M. CD1d-mediated recognition of an α-galactosylceramide by natural killer T cells is highly conserved through mammalian evolution. J Exp Med 1998;188:1521–8.
11. Spada FM, Koezuka Y, Porcelli SA. CD1d-restricted recognition of synthetic glycolipid antigens by human natural killer T cells. J Exp Med 1998;188:1529–34.
12. Nicol A, Nieda M, Koezuka Y, Porcelli S, Suzuki K, Tadokoro K, Durrant S, Juji T. Human invariant $V\alpha24^+$ natural killer T cells activated by α-galactosylceramide (KRN7000) have cytotoxic antitumour activity through mechanisms distinct from T cells and natural killer cells. Immunology 2000;99:229–34.
13. Motohashi S, Kobayashi S, Ito T, Magara KK, Mikuni O, Kamada N, Iizasa T, Nakayama T, Fujisawa T, Taniguchi M. Preserved IFN-γ production of circulating Vα24 NKT cells in primary lung cancer patients. Int J Cancer 2002;102:159–65.
14. Toura I, Kawano T, Akutsu Y, Nakayama T, Ochiai T, Taniguchi M. Cutting edge: inhibition of experimental tumor metastasis by dendritic cells pulsed with α-galactosylceramide. J Immunol 1999;163:2387–91.
15. Akutsu Y, Nakayama T, Harada M, Kawano T, Motohashi S, Shimizu E, Ito T, Kamada N, Saito T, Matsubara H, Miyazawa Y, Ochiai T, et al. Expansion of lung Vα14 NKT cells by administration of α-galactosylceramide-pulsed dendritic cells. Jpn J Cancer Res 2002;93:397–403.
16. Kawano T, Cui J, Koezuka Y, Toura I, Kaneko Y, Motoki K, Ueno H, Nakagawa R, Sato H, Kondo E, Koseki H, Taniguchi M. CD1d-restricted and TCR-mediated activation of Vα14 NKT cells by glycosylceramides. Science 1997;278:1626–9.
17. Kawano T, Cui J, Koezuka Y, Toura I, Kaneko Y, Sato H, Kondo E, Harada M, Koseki H, Nakayama T, Tanaka Y, Taniguchi M. Natural killer-like nonspecific tumor cell lysis mediated by specific ligand-activated Vα14 NKT cells. Proc Natl Acad Sci USA 1998;95:5690–3.
18. Fujii S, Shimizu K, Kronenberg M, Steinman RM. Prolonged IFNγ-producing NKT response induced with α-galactosylceramide-loaded DCs. Nat Immunol 2002;3:867–74.
19. Matsuda JL, Gapin L, Baron JL, Sidobre S, Stetson DB, Mohrs M, Locksley RM, Kronenberg M. Mouse Vα14i natural killer T cells are resistant to cytokine polarization in vivo. Proc Natl Acad Sci USA 2003;100:8395–400.
20. Singh N, Hong S, Scherer DC, Serizawa I, Burdin N, Kronenberg M, Koezuka Y, Van Kaer L. Cutting edge: activation of NK T cells by CD1d and α-galactosylceramide directs conventional T cells to the acquisition of a Th2 phenotype. J Immunol 1999;163:2373–7.
21. Wilson MT, Johansson C, Olivares-Villagomez D, Singh AK, Stanic AK, Wang CR, Joyce S, Wick MJ, Van Kaer L. The response of natural killer T cells to glycolipid antigens is characterized by surface receptor down-modulation and expansion. Proc Natl Acad Sci USA 2003;100:10913–18.
22. Giaccone G, Punt CJ, Ando Y, Ruijter R, Nishi N, Peters M, von Blomberg BM, Scheper RJ, van der Vliet HJ, van den Eertwegh AJ, Roelvink M, Beijnen J, et al. A phase I study of the natural killer T-cell ligand α-galactosylceramide (KRN7000) in patients with solid tumors. Clin Cancer Res 2002;8:3702–9.
23. Nieda M, Okai M, Tazbirkova A, Lin H, Yamaura A, Ide K, Abraham R, Juji T, Macfarlane DJ, Nicol AJ. Therapeutic activation of $V\alpha24^+V\beta11^+$ NKT cells in human subjects results in highly coordinated secondary activation of acquired and innate immunity. Blood 2004;103:383–9.
24. Okai M, Nieda M, Tazbirkova A, Horley D, Kikuchi A, Durrant S, Takahashi T, Boyd A, Abraham R, Yagita H, Juji T, Nicol A. Human peripheral blood $V\alpha24^+$ $V\beta11^+$ NKT cells expand following administration of α-galactosylceramide-pulsed dendritic cells. Vox Sang 2002;83:250–3.
25. Sallusto F, Lanzavecchia A. Efficient presentation of soluble antigen by cultured human dendritic cells is maintained by granulocyte/macrophage colony-stimulating factor plus interleukin 4 and downregulated by tumor necrosis factor alpha. J Exp Med 1994;179:1109–18.
26. Schuler G, Schuler-Thurner B, Steinman RM. The use of dendritic cells in cancer immunotherapy. Curr Opin Immunol 2003;15:138–47.
27. Gunzer M, Janich S, Varga G, Grabbe S. Dendritic cells and tumor immunity. Semin Immunol 2001;13:291–302.
28. Metelitsa LS, Naidenko OV, Kant A, Wu HW, Loza MJ, Perussia B, Kronenberg M, Seeger RC. Human NKT cells mediate antitumor cytotoxicity directly by recognizing target cell CD1d with bound ligand or indirectly by producing IL-2 to activate NK cells. J Immunol 2001;167:3114–22.
29. Exley M, Garcia J, Wilson SB, Spada F, Gerdes D, Tahir SM, Patton KT, Blumberg RS, Porcelli S, Chott A, Balk SP. CD1d structure and regulation on human thymocytes, peripheral blood T cells, B cells and monocytes. Immunology 2000;100:37–47.
30. Salamone MC, Rabinovich GA, Mendiguren AK, Salamone GV, Fainboim L. Activation-induced expression of CD1d antigen on mature T cells. J Leukoc Biol 2001;69:207–14.
31. Kawano T, Tanaka Y, Shimizu E, Kaneko Y, Kamata N, Sato H, Osada H, Sekiya S, Nakayama T, Taniguchi M. A novel recognition motif of human NKT antigen receptor for a glycolipid ligand. Int Immunol 1999;11:881–7.
32. Fujii S, Shimizu K, Steinman RM, Dhodapkar MV. Detection and activation of human $V\alpha24^+$ natural killer T cells using α-galactosyl ceramide-pulsed dendritic cells. J Immunol Methods 2003;272:147–59.
33. Gerosa F, Baldani-Guerra B, Nisii C, Marchesini V., Carra G, Trinchieri G. Reciprocal activating interaction between natural killer cells and dendritic cells. J Exp Med 2002;195:327–33.
34. Cooper MA, Fehniger TA, Fuchs A, Colonna M, Caligiuri MA. NK cell and DC interactions. Trends Immunol 2004;25:47–52.
35. Nestle FO, Alijagic S, Gilliet M, Sun Y, Grabbe S, Dummer R, Burg G, Schadendorf D. Vaccination of melanoma patients with peptide- or tumor lysate-pulsed dendritic cells. Nat Med 1998;4:328–32.
36. Thurner B, Haendle I, Roder C, Dieckmann D, Keikavoussi P, Jonuleit H, Bender A, Maczek C, Schreiner D, von den Driesch P, Brocker EB, Steinman RM, et al. Vaccination with mage-3A1 peptide-pulsed mature, monocyte-derived dendritic cells expands specific cytotoxic T cells and induces regression of some metastases in advanced stage IV melanoma. J Exp Med 1999;190:1669–78.
37. Banchereau J, Steinman RM. Dendritic cells and the control of immunity. Nature 1998;392:245–52.
38. Jonuleit H, Giesecke-Tuettenberg A, Tuting T, Thurner-Schuler B, Stuge TB, Paragnik L, Kandemir A, Lee PP, Schuler G, Knop J, Enk AH. A comparison of two types of dendritic cell as adjuvants for the induction of melanoma-specific T-cell responses in humans following intranodal injection. Int J Cancer 2001;93:243–51.
39. Liu YJ, Kanzler H, Soumelis V, Gilliet M. Dendritic cell lineage, plasticity and cross-regulation. Nat Immunol 2001;2:585–9.
40. Tanaka H, Demeure CE, Rubio M, Delespesse G, Sarfati M. Human monocyte-derived dendritic cells induce naive T cell differentiation into T helper cell type 2 (Th2) or Th1/Th2 effectors. Role of stimulator/responder ratio. J Exp Med 2000;192:405–12.
41. Dhodapkar MV, Geller MD, Chang DH, Shimizu K, Fujii S, Dhodapkar KM, Krasovsky J. A reversible defect in natural killer T cell function characterizes the progression of premalignant to malignant multiple myeloma. J Exp Med 2003;197:1667–76.
42. Tahir SM, Cheng O, Shaulov A, Koezuka Y, Bubley GJ, Wilson SB, Balk SP, Exley MA. Loss of IFN-γ production by invariant NK T cells in advanced cancer. J Immunol 2001;167:4046–50.
43. van der Vliet HJ, Molling JW, Nishi N, Masterson AJ, Kolgen W, Porcelli SA, van den Eertwegh AJ, von Blomberg BM, Pinedo HM, Giaccone G, Scheper RJ. Polarization of $V\alpha24^+$ $V\beta^+$ natural killer T cells of healthy volunteers and cancer patients using α-galactosylceramide-loaded and environmentally instructed dendritic cells. Cancer Res 2003;63:4101–6.
44. Yanagisawa K, Seino K, Ishikawa Y, Nozue M, Todoroki T, Fukao K. Impaired proliferative response of Vα24 NKT cells from cancer patients against α-galactosylceramide. J Immunol 2002;168:6494–9.

THE JOURNAL OF BIOLOGICAL CHEMISTRY
Vol. 280, No. 33, Issue of August 19, pp. 29409–29419, 2005
Printed in U.S.A.

Ras-ERK MAPK Cascade Regulates GATA3 Stability and Th2 Differentiation through Ubiquitin-Proteasome Pathway*[S]

Received for publication, March 2, 2005, and in revised form, June 3, 2005
Published, JBC Papers in Press, June 23, 2005, DOI 10.1074/jbc.M502333200

Masakatsu Yamashita‡, Ryo Shinnakasu‡, Hikari Asou‡, Motoko Kimura‡, Akihiro Hasegawa‡, Kahoko Hashimoto§, Naoya Hatano¶, Masato Ogata¶, and Toshinori Nakayama‡‖

From the ‡Department of Immunology, Graduate School of Medicine, Chiba University, 1-8-1 Inohana Chuo-ku, Chiba 260-8670, the §Department of Life and Environmental Sciences and High Technology Research Center, Chiba Institute of Technology, Narashino, Tsudanuma, Chiba 275-0016, and the ¶Department of Biochemistry, Mie University School of Medicine, 2-174, Edobashi, Tsu, Mie 514-8507, Japan

Differentiation of naive CD4 T cells into Th2 cells requires protein expression of GATA3. Interleukin-4 induces STAT6 activation and subsequent GATA3 transcription. Little is known, however, on how T cell receptor-mediated signaling regulates GATA3 and Th2 cell differentiation. Here we demonstrated that T cell receptor-mediated activation of the Ras-ERK MAPK cascade stabilizes GATA3 protein in developing Th2 cells through the inhibition of the ubiquitin-proteasome pathway. Mdm2 was associated with GATA3 and induced ubiquitination on GATA3, suggesting its role as a ubiquitin-protein isopeptide ligase for GATA3 ubiquitination. Thus, the Ras-ERK MAPK cascade controls GATA3 protein stability by a post-transcriptional mechanism and facilitates GATA3-mediated chromatin remodeling at Th2 cytokine gene loci leading to successful Th2 cell differentiation.

In peripheral lymphoid organs, naive CD4 T cells that have recognized specific antigens differentiate into either one of two distinct helper T cell subsets, Th1 and Th2 cells (1). Upon antigen restimulation, Th1 cells produce large amounts of IFNγ[1] and direct cell-mediated immunity against intracellular pathogens. Th2 cells produce IL-4, IL-5, and IL-13 and are involved in humoral immunity and allergic reactions. The direction of Th cell differentiation depends on the types of cytokine in the environmental milieu (2, 3). Naive CD4 T cells stimulated with antigens in the presence of IL-12 differentiate into Th1 cells, whereas the presence of IL-4 drives differentiation into Th2 cells (4–6). IL-12-mediated activation of signal transducer and activator of transcription (STAT) 4 is crucial for Th1 cell differentiation, and IL-4-mediated STAT6 activation is important for Th2 cell development (7–9).

In addition to the cytokines mentioned above, activation of TCR-mediated signaling is also indispensable for both Th1 and Th2 cell differentiation. We reported that Th2 cell differentiation is highly dependent on the extent of TCR-mediated activation of the p56^{lck}, calcineurin, and Ras-ERK MAPK signaling cascade (10–12). In particular, inhibition of the activation of the Ras-ERK MAPK cascade caused a shift from Th2 to Th1 cell differentiation, suggesting that the direction of Th1/Th2 cell differentiation could be controlled by TCR-mediated activation of the Ras-ERK MAPK cascade (11, 13). On the other hand, Th1 cell development appeared to be regulated by another MAPK, c-Jun N-terminal kinase (14, 15).

Recently, several transcription factors that control Th1/Th2 cell differentiation were identified (8, 16). Among them, GATA3 appears to be a key factor for Th2 cell differentiation. GATA3 is selectively induced in developing Th2 cells after TCR stimulation in the presence of IL-4, and ectopic expression of GATA3 resulted in the induction of Th2 cell differentiation in the absence of STAT6 (17–20). GATA3 was found to be important for the maintenance of the Th2 phenotype (21, 22).

Th2 cell differentiation is accompanied by chromatin remodeling of the Th2 cytokine (IL-4/IL-5/IL-13) gene loci, *e.g.* hyperacetylation of histones H3 and H4 (23–25). Hyperacetylation of the IL-4 and IL-13 gene loci (23) and that of IL-5 gene locus (26) are highly dependent on the expression of GATA3. We described a precise map of the Th2-specific histone hyperacetylation within the Th2 cytokine gene loci, and we identified a 71-bp conserved GATA3-response element at 1.6 kbp upstream of the IL-13 locus (23). The GATA3-response element appears to play a crucial role for GATA3-mediated targeting and downstream spreading of core histone hyperacetylation within the IL-13 and IL-4 gene loci in developing CD4$^+$ Th2 and CD8$^+$ Tc2 cells (23, 27).

One of the major pathways of degradation of short lived regulatory proteins, including transcriptional factors, is through ubiquitin-mediated targeting and protein destruction in the 26 S proteasome. Protein ubiquitination is involved in a wide range of cellular processes, including cell cycle progression, signal transduction, transcriptional regulation, DNA re-

* This work was supported by grants from the Ministry of Education, Culture, Sports, Science and Technology (Japan), Grants-in-aid for Scientific Research Priority Areas Research 13218016 and 16043211, Scientific Research B 14370107, Scientific Research C 16616003 and 15790248, and Special Coordination Funds for Promoting Science and Technology, the Ministry of Health, Labor, and Welfare (Japan), the Program for Promotion of Fundamental Studies in Health Science of the Organization for Pharmaceutical Safety and Research (Japan), The Japan Health Science Foundation, Uehara Memorial Foundation, and Mochida Foundation. The costs of publication of this article were defrayed in part by the payment of page charges. This article must therefore be hereby marked "*advertisement*" in accordance with 18 U.S.C. Section 1734 solely to indicate this fact.

[S] The on-line version of this article (available at http://www.jbc.org) contains Fig. 1.

‖ To whom correspondence should be addressed: Dept. of Immunology (H3), Graduate School of Medicine, Chiba University, 1-8-1 Inohana, Chuo-ku, Chiba, 260-8670 Japan. Tel.: 81-43-226-2200; Fax: 81-43-227-1498; E-mail: tnakayama@faculty.chiba-u.jp.

[1] The abbreviations used are: IFNγ, interferon-γ; dn, dominant-negative; ERK, extracellular signal-regulated kinase; Erk2 sem., an active form of ERK2; KO, knock out (deficient); Tg, transgenic; Ub, ubiquitination; WT, wild type; TCR, T cell receptor; STAT, signal transducer and activator of transcription; IL, interleukin; PMA, phorbol 12-myristate 13-acetate; mAb, monoclonal antibody; ChIP, chromatin immunoprecipitation; MAPK, mitogen-activated protein kinase; MEK, MAPK/ERK kinase; siRNA, small interfering RNA; CHX, cycloheximide; GFP, green fluorescent protein; EGFP, enhanced GFP; hNGFR, human nerve growth factor receptor p75; FCS, fetal calf serum; E3, ubiquitin-protein isopeptide ligase.

pair, antigen presentation, and apoptosis (28–31). Emerging views suggest that various aspects of the immune system are controlled by ubiquitination (32). A well known example of the ubiquitin-dependent regulation in the immune system is the proteasome-dependent processing of peptides in antigen-presenting cells (33). It is also well known that lipopolysaccharide or proinflammatory cytokines such as IL-1 can induce activation of NF-κB through ubiquitination and subsequent degradation of the inhibitor of κB (34). However, a role for the ubiquitin-mediated regulation of Th1/Th2 cell differentiation has not been reported.

In the present study, we investigated the molecular targets of the Ras-ERK MAPK cascade that control chromatin remodeling of the Th2 cytokine gene loci and subsequent Th2 cell differentiation, and we found that the Ras-ERK MAPK cascade controls the stability of the GATA3 protein through the ubiquitin-proteasome pathway. Moreover, we demonstrated that the ubiquitination of GATA3 by Mdm2 is dependent on a ring finger domain.

EXPERIMENTAL PROCEDURES

Mice—C57BL/6 mice were purchased from SLC (Shizuoka, Japan). STAT6-deficient (KO) mice were kindly provided by Shizuo Akira (Osaka University, Osaka, Japan) (35). A T cell-specific H-ras dominant-negative (dnRas) transgenic (Tg) mouse with the *lck* proximal promoter was described elsewhere (11, 36). All mice used in this study were maintained under specific pathogen-free conditions.

Reagents—PD98059 (Calbiochem), cycloheximide (Calbiochem), MG132 (Sigma), and U0126 (Promega) were purchased.

Expression Plasmids and Transfection—Myc-tagged and FLAG-tagged GATA3 mutants (pCMV Tag 3B-GATA3 WT, dCT, dCF, and dZF), and GFP-fused GATA3 mutants (pEGFP-C1 GATA3 WT and pEGFP-C1 GATA3 dZF) were generated by PCR-based mutation. Myc-tagged wild type Mdm2, RING finger-deleted Mdm2 (pCMV Tag-3B-Mdm2 WT, dR), and $p19^{ARF}$ were generated in our laboratory. COS, 293T, and NIH3T3 cells were transfected using FuGENE reagent (Invitrogen) according to the manufacturer's protocol.

Cell Cultures and in Vitro T Cell Differentiation—CD4 T cells were purified using magnetic beads and an auto-MACS® sorter (Miltenyi Biotec), yielding a purity of >98%. The purified CD4 T cells (1.5×10^6) were stimulated for 2 days with immobilized anti-TCR mAb (H57–597, 3 μg/ml) in the presence of IL-2 (25 units/ml), IL-12 (100 units/ml), and anti-IL-4 mAb (11B11, 25% culture supernatant) for Th1-conditions or in the presence of IL-2 (25 units/ml), IL-4 (100 units/ml), and anti-IFNγ mAb (R4.6A2, 25% culture supernatant) for Th2− conditions. The cells were cultured for another 3 days in the presence of only the cytokines present in the initial culture. The numbers of Th1/Th2 cells were determined by using intracellular staining with anti-IL-4 and anti-IFNγ as described (10).

Retroviral Vectors and Infection—pMX-IRES-CAR (human coxsackie-adenovirus receptor) plasmid was generated from the pMX-IRES-GFP plasmid by replacing the EGFP gene with the CAR gene. The methods for the generation of virus supernatant and the infection were described previously (37). Infected cells were subjected to intracellular staining with anti-IL-4 and anti-IFNγ mAb or to cell sorting. To prepare large numbers of infected cells for immunoblotting, the pMX-IRES-CAR or pMXs-IRES-hNGFR vector was used, and the infected cells were enriched by auto-MACS® sorter with anti-CAR mAb (38) or anti-human NGFR (C40–1457; Pharmingen). cDNA encoding Erk2 sem was described previously (39). pMXs-Mdm2 dR-hNGFR was constructed by inserting Mdm2-dR into a multicloning site of pMXs-IRES-hNGFR. cDNA for human GATA3 or an active form of human Raf-1 (40) was inserted into a multicloning site of pMX-IRES-GFP.

Chromatin Immunoprecipitation (ChIP) Assay—ChIP was performed using the histone H3 assay kit (catalog number 17-245; Upstate Biotechnology, Inc.) as described previously (23). Semi-quantitative PCR was performed with DNA samples from 3 or 1×10^4 cells at 28 cycles. PCR products were resolved in an agarose gel and visualized by ethidium bromide. Images were recorded and quantified using ATTO L & S analyzer (ATTO, Tokyo, Japan). The primers used were described previously (23).

Immunoprecipitation and Immunoblotting—Purified CD4 T cells were stimulated with immobilized anti-TCR mAb for 2 days as described above, and nuclear extracts were prepared with an NE-PER™ nuclear and cytoplasmic extract reagent (catalog number 78833; Pierce) according to the manufacturer's protocol. The amount of GATA3, c-Maf, or α-tubulin was assessed by immunoblotting with anti-GATA3 mouse mAb (HG3–31; Santa Cruz Biotechnology, Santa Cruz, CA), anti-c-Maf rabbit antisera (M-153; Santa Cruz Biotechnology), or anti-α-tubulin mAb (DM1A; Lab Vision Corp.) as described previously (37). Anti-Mdm2 mAb (D-17; Santa Cruz Biotechnology), anti-E6-AP mAb (clone 20; BD Transduction Laboratories), anti-Itch mAb (clone 32; BD Transduction Laboratories), and anti-Cbl-b mAb (G-1; Santa Cruz Biotechnology) were used for immunoblotting. For transfectants, anti-FLAG mAb (M2; Sigma) and anti-Myc mAb (PL14; MBL) were used for immunoblotting.

For anti-ubiquitin blotting, COS cells were transfected with Myc-tagged GATA3 vectors (pCMV Tag 3B). Two days later, cells were treated with cycloheximide (100 μM) and U0126 (20 μM) in the presence or absence of the proteasome inhibitor MG132 (50 μM) for 2 h. The cells were then pelleted, resuspended in RIPA buffer, and lysed on ice for 30 min. Insoluble material was removed by centrifugation. The lysates were incubated with 5 μg of anti-Myc mAb (MBL, Japan) for 2 h at 4 °C. 50 μl of protein G-conjugated Sepharose (Amersham Biosciences) was then added and incubated for an additional 1 h. After removal of the supernatant, the beads were washed twice with RIPA buffer. The bound protein was eluted by adding 25 μl of SDS sample buffer and was subjected to immunoblot analysis using mAb specific for ubiquitin (FK2; MBL, Tokyo, Japan).

Northern Blotting—Total RNA (20 μg) was isolated from cultured cells using TRIzol reagent (Invitrogen), separated on a 1% formaldehyde gel, and transferred to a Nytran Plus membrane (Schleicher & Schuell). Probes for GATA3 and β-actin were generated by PCR using the primers described previously (37). The digoxigenin labeling and detection system (Roche Diagnostics) was used for visualization.

Pulse-Chase Experiment—Splenic CD4 T cells were stimulated for 2 days under Th2− conditions. The cells were washed, preincubated for 30 min in methionine/cysteine-free medium, and pulsed for 30 min with 200 μCi/ml [^{35}S]methionine/cysteine (ICN). Then the cells were washed twice with Dulbecco's modified Eagle's medium containing nonradioactive 5 mM L-methionine, 3 mM L-cysteine, and 0.25% FCS, and chased in the same medium in the presence of PMA (3 ng/ml) or PMA plus U0126 (20 μM). U0126 was used in the pulse-chase experiment because it is known to inhibit preactivated MEK as well (41).

In Vitro Ubiquitination Assay—*In vitro* ubiquitination assay was performed as described previously (42). In brief, 293T cells were transfected with FLAG-tagged GATA3, and 3 days later the cells were treated with MG132 for 2 h. Then the cells were lysed in RIPA buffer (2.5×10^6 cells/ml), and the cell lysates (250 μl) were subjected to immunoprecipitation with anti-FLAG or anti-GATA3 mAb. The immunoprecipitates were incubated for 2 h at 30 °C in 25 μl of reaction buffer containing 50 mM Tris-HCl (pH 8.0), 50 ng of recombinant mouse ubiquitin-activating enzyme, 500 ng of ubiquitin carrier protein, 5 μg of glutathione *S*-transferase-Ub, 1 mM dithiothreitol, 2 mM $MgCl_2$, and 4 mM ATP. After terminating the reaction by the addition of 2× SDS sample buffer, immunoblotting with anti-GATA3 or anti-FLAG mAb was performed. Recombinant mouse ubiquitin-activating enzyme, ubiquitin carrier protein, and glutathione *S*-transferase-Ub were kindly provided by Dr. Keiji Tanaka (Tokyo Metropolitan Institute for Medical Science, Tokyo, Japan).

siRNA—Introduction of siRNA into a T cell line TG40 was performed as described (43). In brief, 2 μl of TransIT-TKO transfection reagent (Mirus) was diluted in 50 μl of serum-free/antibiotic-free RPMI 1640 per well. Ten minutes later, 1 μl of 40 μM siRNA was added to the diluted transfection reagent and incubated for 30 min with gentle agitation. Then the siRNA solution was added to TG40 cultures containing 5×10^5 cells in 500 μl of medium per well in a 24-well plate. Three days after transfection, ubiquitination of GATA3 and the expression of Mdm2 protein were assessed by immunoblotting. Pre-designed siRNA for Mdm2 was purchased from Ambion (16704), and control siRNA was from Santa Cruz Biotechnology (sc-37007).

RESULTS

The Ras-ERK MAPK Cascade Controls Histone Hyperacetylation of the Th2− Cytokine Gene Loci—We reported that Th2 cell differentiation and certain Th2 responses are dependent on the extent of activation of the Ras-ERK MAPK cascade (11, 13). Hyperacetylation of the Th2 cytokine gene loci was highly dependent on the expression of GATA3 (23, 26). We present here further confirmation of the observations in chromatin remodeling of the Th2 gene loci. The generation of IL-4-produc-

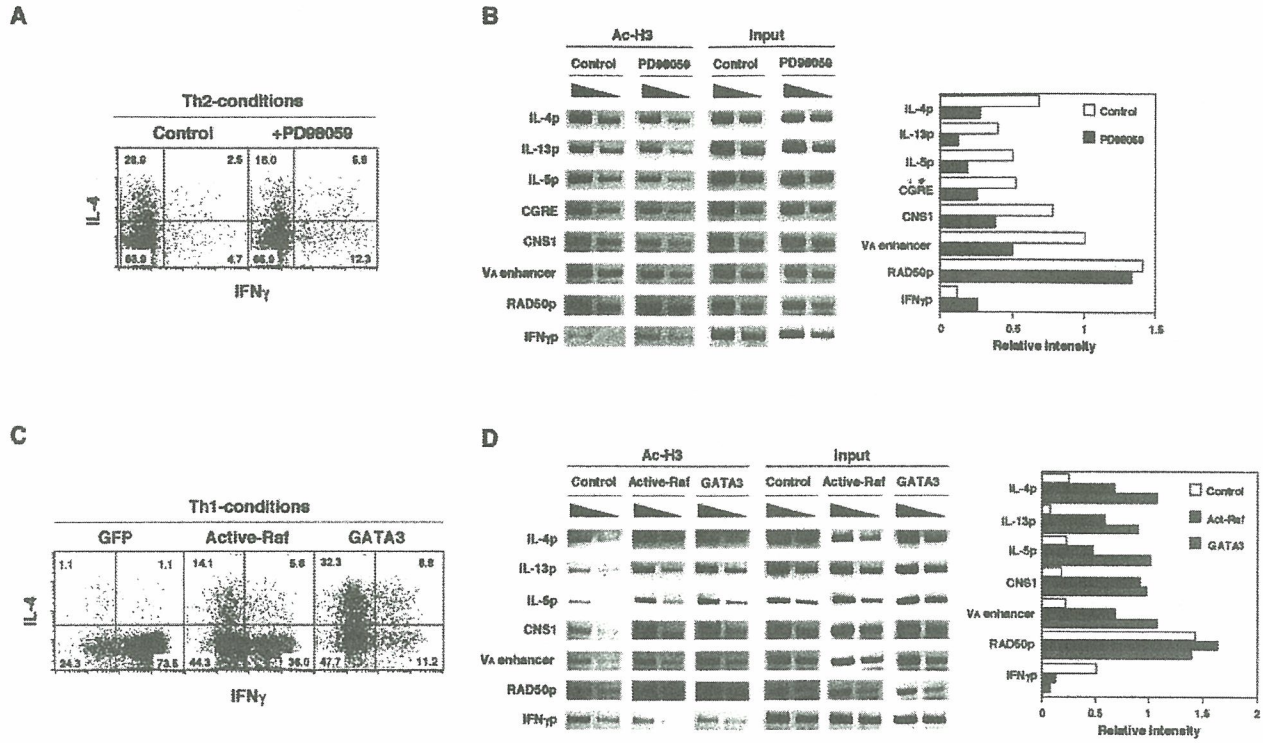

FIG. 1. **Activation of the ERK-MAPK cascade is required for GATA3-dependent histone H3 hyperacetylation of Th2 cytokine gene loci.** *A*, Th2 cell differentiation was inhibited by PD98059, a specific inhibitor of MEK. Freshly prepared splenic CD4 T cells were stimulated under Th2− conditions in the presence of PD98059 (30 μM) for 2 days. The cells were cultured for an additional 3 days and then stimulated with immobilized anti-TCR mAb. The numbers of Th1/Th2 cells were determined by intracellular staining with anti-IL-4 and anti-IFNγ. The *numbers* represent the percentages of cells in each quadrant. *B*, the effect of PD98059 on the histone H3 hyperacetylation. An aliquot of the cells cultured as in *A* were harvested on day 3, and the acetylation status of histone H3 in nucleosomes associated with the indicated regions was assessed by ChIP assay. An anti-acetylated histone H3 (K9, K14) antibody and specific primer pairs were used. Three independent experiments were performed, and similar results were obtained. Relative band intensities normalized by input DNA bands measured by a densitometer are shown in the *right panel*. *C*, expression of active Raf-induced IL-4 producing Th2 cells under Th1− conditions. Freshly prepared splenic CD4 T cells were stimulated under Th1− conditions and infected with retrovirus encoding active Raf or GATA3 bicistronically with EGFP on day 2. Three days later, the cells were stimulated with anti-TCR and were subjected to IL-4/IFNγ staining. *D*, histone H3 hyperacetylation on Th2 cytokine gene loci was induced by an active form of Raf-1 (*Active-Raf*) or ectopic expression of GATA3 in developing Th1 cells. GFP-positive infected CD4 T cells were enriched by cell sorting. *Control* represents mock vector virus infection. Acetylation status of histone H3 was determined by ChIP assay. Three independent experiments were done with similar results. Relative band intensities normalized by input DNA bands are shown in the *right panel*.

ing cells was substantially inhibited in the presence of a specific inhibitor of MEK (an ERK MAPKK), PD98059 (Fig. 1*A*). Fig. 1*B* shows that the acetylation levels of histones associated with the Th2 cytokine gene loci (IL-4 promoter, IL-13 promoter, IL-5 promoter, GATA3-response element, CNS1, and IL-4 V_A enhancer) were significantly reduced in the presence of PD98059. In the case of RAD50, there was no significant effect with PD98059 treatment, and with the IFNγ promoter (IFNγp) there was some enhancement in the acetylation. Under Th1 culture conditions, PD98059 exhibited no detectable inhibition of acetylation at the IFNγ promoter region (data not shown).

In addition, the effect of ectopic expression of an active form of Raf-1 (active-Raf) on the generation of Th1/Th2 cells was assessed. Significant numbers of IL-4-producing Th2 cells and a suppression of the generation of IFNγ-producing cells were observed in active Raf-infected cells stimulated under Th1− conditions (Fig. 1*C*). As a positive control, GATA3 infection was included, and in this case substantial levels of IL-4-producing cells with decreased numbers of IFNγ-producing cells were detected. Assessment of the acetylation status of histones in the active Raf-infected or GATA3-infected T cells defined by GFP expression on day 2 revealed significant increases in acetylation at the IL-4, IL-13, and IL-5 promoters and CNS1 and IL-4 V_A enhancer regions; however, the effect on the RAD50 promoter region was marginal (Fig. 1*D*). A significant decrease in the acetylation of the IFNγ promoter region was observed in the presence of active Raf. The levels of acetylation induced by active Raf infection were lower than those induced by GATA3. A possible explanation for this could be the limited expression of GATA3 in T cells cultured under Th1− conditions. Nevertheless, it is clear that the ERK-MAPK cascade controls GATA3-dependent histone hyperacetylation of the Th2 cytokine gene loci in developing Th2 cells.

Activation of the Ras-ERK MAPK Cascade Is Required for Stable Expression of GATA3 Protein in Developing Th2 Cells—GATA3 is a critical transcriptional factor for Th2 cell differentiation (17–19), and its expression is induced selectively under Th2− conditions. Here we demonstrate this in freshly prepared splenic CD4 T cells stimulated under Th1 and Th2 conditions (Fig. 2*A*, compare *lanes 1* and *3* and *lanes 2* and *4*). Treatment of Th2 condition cultures with PD98059 resulted in decreased protein expression of GATA3 (Fig. 2*A*, *lanes 5* and *6*). Similarly, the induction of GATA3 protein in dominant-negative Ras (dnRas) Tg T cells was significantly lower than that seen in the control, and this is consistent with the observation of impaired Th2 cell differentiation in dnRas Tg mice (11). A specific inhibitor for the p38 MAPK cascade (SB203580) did not affect the GATA3 expression in developing Th2 cells (data not shown). The activation of STAT6 is known to be critical for GATA3 transcription, and as expected, STAT6-deficient (STAT6 KO) CD4 T cells failed to induce GATA3 protein.

Concurrently, the transcriptional levels of GATA3 in T cells

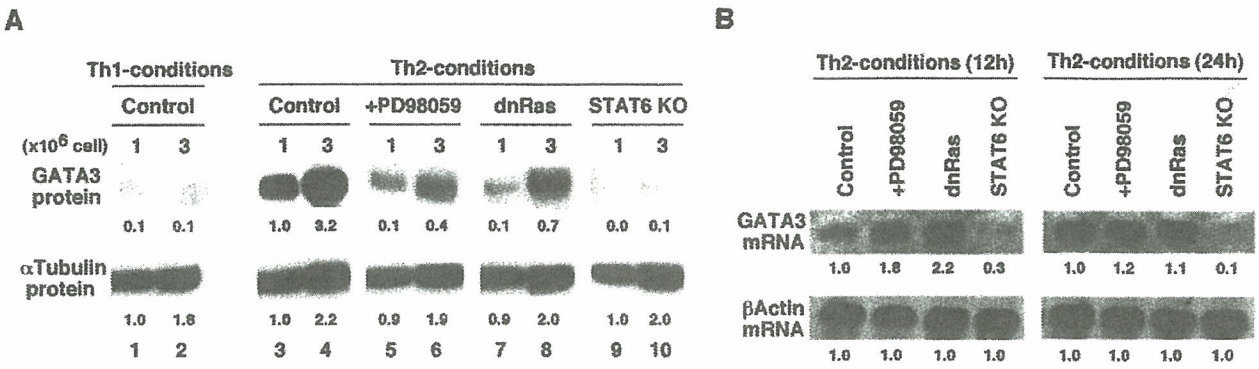

FIG. 2. **Activation of the ERK-MAPK cascade controls GATA3 protein expression without inhibiting transcription in developing Th2 cells.** *A*, ERK MAPK- and STAT6-dependent expression of GATA3 protein. Freshly prepared splenic CD4 T cells were stimulated under the indicated conditions for 2 days, and the expression of GATA3 protein in nuclei was assessed. CD4 T cells from T cell-specific dominant-negative H-Ras (dnRas) Tg mice and STAT6-deficient (STAT6 KO) mice were also used. The expression of α-tubulin was assessed as a control. A representative result from one of three independent experiments is shown. Arbitrary densitometric units normalized with α-tubulin bands are shown below each band. *B*, no effect of inhibition of the ERK-MAPK cascade on the transcriptional up-regulation of GATA3. Splenic CD4 T cells were stimulated under Th2− conditions for 12 and 24 h, and the expression levels of GATA3 mRNA were determined by Northern blot analysis. To examine the role for ERK-MAPK cascade activation, PD98059 (30 μM) and the CD4 T cells from dnRas Tg mice were used. Three independent experiments were performed with similar results. Arbitrary densitometric units are shown below each band.

cultured under Th2 conditions (12 and 24 h) as in Fig. 2*A* were assessed (Fig. 2*B*). The inhibition of activation of the Ras-ERK MAPK cascade by PD98059 or overexpression of dnRas transgene in T cells had no blocking effect on GATA3 mRNA expression. Rather, significant enhancement of GATA3 levels was detected at the 12-h time point. In contrast, GATA3 mRNA was not induced to significant levels in STAT6-deficient CD4 T cells, which is consistent with the lack of induced GATA3 protein.

Consequently, we sought to investigate further the consequence of the inhibition of ERK MAPK activation on the degradation of GATA3 protein. Splenic CD4 T cells were first stimulated under Th2− conditions for 2 days prior to being cultured without IL-4 or immobilized anti-TCR mAb for various time periods (chase) in either the presence or absence of another specific MEK inhibitor (U0126), which is also effective on activated MEK (Fig. 3, *A* and *B*). Under normal culture conditions with 10% FCS, the levels of GATA3 protein remained elevated over 12 h but then they declined significantly at 24 h. In the presence of U0126, significant reduction of GATA3 protein was observed at the 6- and 12-h time points, and the protein was virtually undetectable after a 24-h chase (Fig. 3*A*). U01126 treatment did not affect the level of another Th2-specific transcription factor, c-Maf. Under culture conditions with low levels of FCS (0.25%), where decreased levels of background stimulation of the MAPK cascades were detected (data not shown), a gradual decrease in GATA3 protein was seen and a modest rescue by the presence of PMA was observed (Fig. 3*B*). In the presence of U0126, the loss of GATA3 protein was dramatic, and GATA3 was barely detectable at the 12- and 24-h time points.

As an alternative means to assess the effect of ERK MAPK on the stability of the GATA3 protein, we performed pulse-chase experiments to follow the degradation of GATA3, and we found that the amount of ^{35}S-labeled nascent GATA3 protein was degraded very rapidly in the presence of U0126 (Fig. 3*C*). These results clearly demonstrate that rapid degradation of GATA3 occurs when activation of ERK MAPK is inhibited.

As a more direct test of the requirement for the activation of ERK MAPK to stabilize GATA3 in developing Th2 cells, we introduced an active form of ERK2 (Erk2 sem) (39) or a dominant-negative form of ERK2 (dnErk2) (44) into developing Th2 cells (Fig. 3*D*). As anticipated, GATA3 protein was significantly retained in cells infected with ERK2 sem, whereas the expression of dnERK2 significantly enhanced its degradation. Thus, the stability of GATA3 protein in developing Th2 cells appears to be highly dependent on the activation of the Ras-ERK MAPK cascade.

GATA3 Is Rapidly Degraded through the 26 S Proteasome Pathway—It would seem very likely that the proteasome pathway would be involved. To determine whether the 26 S proteasome is involved with the rapid degradation of the GATA3 protein, the effect of a proteasome inhibitor MG132 was examined. COS cells were transfected with Myc-tagged GATA3 and treated with cycloheximide (CHX) to inhibit protein synthesis in the presence or absence of MG132 for 1 or 2 h. Myc-tagged GATA3 was predominantly expressed in the nucleus, and after CHX treatment it was degraded rapidly in the absence of MG132 (Fig. 4*A*, *left panel*). In contrast, in the presence of MG132, there was a dramatic increase in the amount of Myc-tagged GATA3 protein in both nuclear and cytoplasmic fractions (Fig. 4*A*, *right panel*). Moreover, in developing Th2 cells GATA3 protein was degraded rapidly in the presence of CHX, and the degradation was inhibited by MG132 (Fig. 4*B*). In addition, another proteasome inhibitor lactacystin was tested in primary T cells for its ability to affect the degradation of GATA3, and a significant blocking of the degradation of GATA3 was observed (Fig. 4*C*). Collectively, these results point to the involvement of the 26 S proteasome pathway in the degradation of GATA3.

The C-terminal Region of GATA3 Including the Zinc Finger Domain Is Critical for Proteasome-dependent Degradation—In an attempt to map the target region of GATA3 that is critical for proteasome-dependent degradation, we prepared several truncated GATA3 mutants of the N-terminal region, which contains many lysine residues that can be ubiquitinated (Fig. 4*D*). Myc-tagged wild type (WT), dCT, dCF, and dZF constructs were transfected into COS cells, and the expression levels of GATA3 were assessed after treatment with MG132 (Fig. 4*E*). In comparison to wild type GATA3, there was essentially no difference in the pattern of disappearance of either the dCT or dCF mutant forms from nuclear fractions following CHX treatment, or in the retention of GATA3 protein by MG132 treatment. In the cytosol fraction of transfectants without drug treatment, slightly increased levels of protein were detected with dCT and dCF mutants, but the levels after treatment with MG132 were indistinguishable (Fig. 4*E*, *lower panels*). In sharp contrast, large amounts of dZF mutant protein were detected in

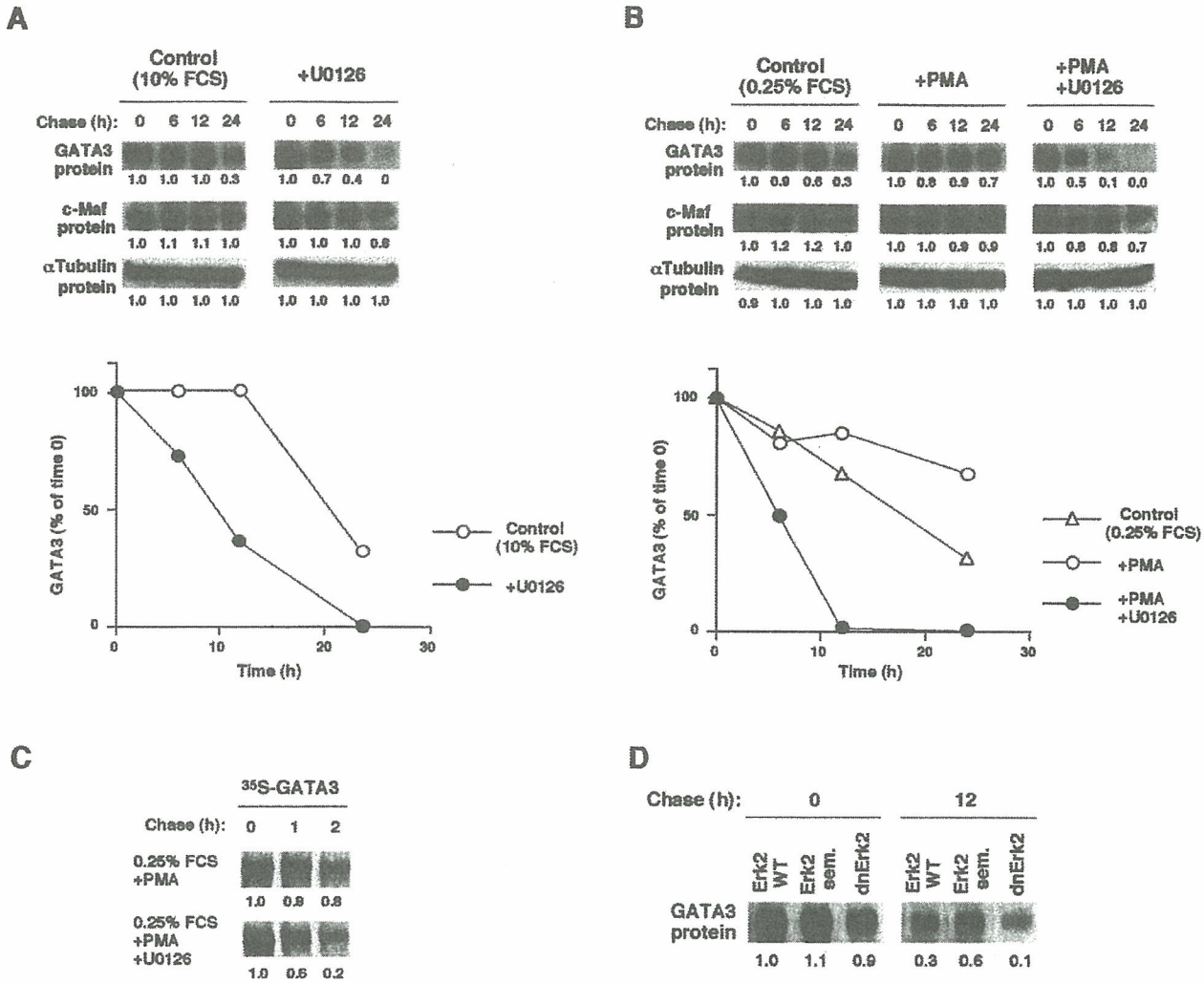

FIG. 3. **Regulation of the expression of GATA3 protein in developing Th2 cells by the ERK-MAPK cascade.** *A*, inhibition of ERK MAPK activation induces GATA3 protein degradation. Splenic CD4 T cells were stimulated under Th2− conditions for 2 days. The cells were then cultured for 6 and 12 h without cytokines in the presence or absence of MEK inhibitor U0126 (20 μM) with 10% FCS in the medium. The expression of GATA3 protein was assessed as in Fig. 2*A*. The expression of c-Maf and α-tubulin protein was also determined as controls. Arbitrary densitometric units are shown below each band, and the percentages of each point are shown in a *graph*. Three independent experiments with different time courses were performed with similar results. *B*, GATA3 protein degradation in the presence of PMA and U0126. Splenic CD4 T cells were stimulated for 2 days as described in *A*. Then the cells were cultured in the presence of PMA (3 ng/ml) and U0126 (20 μM) with just 0.25% FCS in the medium. The protein expression levels of GATA3, c-Maf, and α-tubulin protein were examined. Three independent experiments were performed, and a representative result is shown. *C*, degradation of GATA3 determined by pulse-chase analysis. Splenic CD4 T cells were stimulated as described in *A*. Then the cultured cells were labeled with [^{35}S]methionine and [^{35}S]cysteine and chased in a medium containing 0.25% FCS, nonradioactive methionine and cysteine in the presence or absence PMA (3 ng/ml). The effect of U0126 was examined. ^{35}S-Labeled GATA3 protein was visualized by autoradiography. Arbitrary densitometric units are shown below each band. Three independent experiments were performed, and a representative result is shown. *D*, effect of an active form of ERK2 (Erk2 sem) and a dominant-negative form of ERK2 (dnErk2) on the expression of GATA3. Splenic CD4 T cells were stimulated as described in *A*, and the cells were infected with retrovirus encoding ERK2 mutant bicistronically with human coxsackievirus and adenovirus receptor (*CAR*). Three days after infection, the coxsackievirus and adenovirus receptor-positive population was enriched by MACS and cultured at 37 °C for 12 h without cytokines. Then the expression levels of GATA3 protein were assessed. Arbitrary densitometric units are shown below each band. Four independent experiments were performed, and a representative result is shown.

the cytosol, and treatment with either CHX or MG132 did not have a significant effect on the levels of the mutant protein. Small amounts of dZF protein were detected in the nuclear fraction, and a modest increase was detected in the presence of MG132. Thus it would appear the C-terminal region of GATA3, including the zinc finger region (residues 261–315), is critical for proteasome-dependent degradation.

To visualize the dynamics of localization and accumulation, green fluorescence protein (GFP)-fused wild type GATA3 and the dZF mutant were expressed in NIH3T3 cells. As expected, wild type GATA3 showed decreased fluorescence following CHX treatment, and the decrease in fluorescence was prevented to some extent in the presence of MG132 (supplemental Fig. 1). The dZF mutant was expressed in both nuclear and cytosolic fractions, and the fluorescence intensity was not affected by treatment with CHX or MG132. These results are consistent with the results shown in Fig. 4*C*.

The ERK MAPK Cascade Regulates GATA3 Ubiquitination—In order to assess the involvement of multiubiquitination (Ub) in GATA3 degradation, FLAG-tagged wild type GATA3, dCT, dCF, and dZF mutants were each transfected into 293T cells, and transfectants were treated with MG132. Immuno-